THE UNIVERSITY OF CALGARY

A PROTOTYPE MULTI-STATION, MULTI-PASS GPS SATELLITE DATA REDUCTION PROGRAM

BY

BRENT A. WANLESS

A THESIS

SUBMITTED TO THE FACULTY OF GRADUATE STUDIES
IN PARTIAL FULFILLMENT OF THE REQUIREMENTS FOR THE
DEGREE OF MASTER OF SCIENCE IN ENGINEERING

DEPARTMENT OF CIVIL ENGINEERING
Division of Surveying Engineering

CALGARY, ALBERTA
AUGUST, 1985

THE UNIVERSITY OF CALGARY

FACULTY OF GRADUATE STUDIES

The undersigned certify that they have read, and recommend to the Faculty of Graduate Studies for acceptance, a thesis entitled, "A Prototype Multi-station, Multi-pass GPS Satellite Data Reduction Program", submitted by Brent A. Wanless in partial fulfillment of the requirements for the degree of Master of Science in Engineering.

Chairman, Dr. E. J. Krakiwsky
Department of Civil Engineering
Division of Surveying Engineering

K.P. Schwarz.

Dr. K. P. Schwarz
Department of Civil Engineering
Division of Surveying Engineering

Dr. S. M. Nakiboglu
Department of Civil Engineering
Division of Surveying Engineering

Dr. E. F. Milone
Department of Physics

August 20, 1985

ABSTRACT

The development of a prototype, multi-station, multi-pass GPS satellite data reduction program is presented in this thesis. The prototype program utilizes simulated observations to perform orbit improvement and station coordination, either simultaneously or independantly.

The observation equations for pseudorange, continuously integrated Doppler and single difference phase measurements are given. The adjustment model, which has a weighted least squares collocation form, is formulated and the adjustment equations derived. Two possible tracking network configurations are presented for orbit improvement over Canada. Results are presented for simulation tests which show the ability to improve the accuracy of GPS satellite orbits to an accuracy of 2.5 m . Results are also presented for the solution of receiver clock errors, and local station coordinates using broadcast ephemerides and improved orbits.

ACKNOWLEDGEMENTS

The completion of the research for my thesis would not have been possible without the advice and encouragement I received from many people. The insight and enthusiasm provided by my supervisor, Dr. E.J. Krakiwsky, generated the drive necessary to complete this work, and his support is acknowledged. I would also like to acknowledge Dr. K.P. Schwarz and Dr. S.M. Nakiboglu for their help with various technical problems.

I would like to thank all my fellow graduate students for the help provided through useful discussions and debates on various topics. In particular, Bruce Buffett, who was also in the research group, and Phil Mackenzie, for assisting me with the VAX word processing system used to prepare this document. I sincerely thank my parents, for without their support in past years I would not have even contemplated attempting this level of education. Finally, I would like to thank Dimitra, for encouraging and supporting me in her own special way.

The research undertaken for this thesis was performed in conjunction with, and partially funded by, a research contract with the Geodetic Survey of Canada. The cooperation of the contract supervisor, Dr. D. Delikaraoglou, is also acknowledged. Financial support also came from the Natural Sciences and Engineering Research Council of Canada in the form of an NSERC postgraduate scholarship; the Division of Surveying Engineering of the University of Calgary; and the Walker Newby and Associates Ltd award.

TABLE OF CONTENTS

LIST OF TABLES

LIST OF FIGURES

GLOSSARY

• ambiguity parameter	the unknown integer number of wavelengths arising when single difference observations are formed
• broadcast ephemeris	the parameters encoded in the broadcast satellite message defining the satellite arc
• Doppler measurement	the observation formed by counting the beats produced when differencing a reference frequency and a frequency changing due to Doppler shift
• Keplerian initial conditions	the six Keplerian parameters defining a satellite pass at a reference epoch
• mathematical model	a function relating unknown parameters to measured values
• NNSS	Navy Navigation Satellite System
• nuisance parameter	an unknown quantity to be solved that is not of prime interest
• precise ephemeris	an accurate representation of a satellite pass, generally produced post-mission
• pseudorange	the range measurement possible from GPS satellites that is biased due to clock synchronization error
• range bias	the unknown range at lock-on time associated with Doppler measurements processed in a continuously integrated manner
• relative positioning	the determination of coordinate differences between stations rather than coordinate values

• single difference	the observation formed by differencing a satellite signal received simultaneously at two stations

CHAPTER 1

INTRODUCTION

The establishment of relative station positions is a common geodetic task. Classically, the techniques of triangulation, trilateration and traversing have been used to determine relative positions. In the early 1970's, application of the Transit Doppler satellite system (NNSS) to relative positioning work proved to be extremely powerful [Brown,1970]. The main advantages of satellite based systems are they do not require line-of-sight between stations, and they can be operated under virtually all weather conditions. The accuracy achievable with Transit observations is on the order of a few metres for point positioning, and a few decimetres for relative positioning [Wells et al.,1976]. To achieve these accuracies, however, a long observation period is required since Transit satellite coverage is quite limited, and many passes are required to increase geometrical strength and redundancy. In the late 1970's, the Global Positioning System (GPS) of satellites entered the phase I development and testing stage [Milliken and Zoller,1978]. The fully operational system of 18 GPS satellites will have three main advantages over the Transit system: 1) there will be at least four satellites available to users 24 hours a day, virtually everywhere on the earth; 2) along with Doppler and phase measurements, the satellite emitted code allows for pseudorange measurements not possible with Transit satellites;and 3) the high satellite altitude provides for longer observing time spans. These advantages have already proven that GPS can provide better relative positioning accuracies in a shorter observation time than the Transit system [Bock et al.,1985].

The positioning results from GPS reported to date have involved observations of pseudorange, Doppler, and various differences of carrier phase to produce single point coordinates and relative station coordinate differences. The computer software used has been developed by many different groups, however, there are similarities in their approaches. Generally, the satellite coordinates required for computations are assumed to be known and treated as errorless, or else biases for each pass are solved for. The coordinate values are either computed from the broadcast ephemeris message, or input from a precise ephemeris file. Also, the solution is usually performed for a single station or, in a relative positioning mode, for a single baseline at a time. More recent and modern software development has allowed for the processing of multiple baselines simultaneously as more receivers are deployed in the field during the same observing schedule.

The research reported in this thesis is on the development of a prototype GPS adjustment program, which can handle multiple satellite passes and multiple observing stations simultaneously. The program utilizes either pseudorange, Doppler, or single difference phase observations. The satellite position computations are based on numerical integration of the equations of motion for the satellite under the adopted force model . The adjustment formulation is a rigorous, weighted least-squares approach, allowing for adjustment of the satellite reference initial conditions along with station coordinate determination and solution of other nuisance parameters. The formulation also yields complete covariance matrices for the satellite and station solutions through rigorous covariance propagation.

1.1 Precise Relative Positioning

The ability to produce accurate relative positions quickly and economically with GPS has rapidly made this system a powerful geodetic tool. It may not be far in the future when geodetic networks are established and maintained solely with GPS techniques. The current system is routinely providing 1 to 2 ppm relative accuracies on baselines up to 200 km in length [Goad and Remondi,1984 ; Beck et al., 1984]. This level of accuracy is being achieved using carrier phase and/or pseudorange measurements taken over a few hours.

Significant advances in the study of geophysical processes have been made with recent improvements in Long Baseline Interferometry (LBI) technology. The accuracy of LBI solutions is on the order of 1 part in 10^{-8} and better, allowing for accurate determinations of polar motion, earth rotation rate and crustal motion. The use of GPS for monitoring crustal motion may be possible on a regional scale, however, the relative accuracies of 0.1 ppm that are required have not been achieved to date. A 0.1 ppm level of accuracy would also be beneficial for precise geodetic work, where eventually a unified and accurate worldwide geodetic reference frame could be established.

1.2 Orbit Improvement

The relative positioning accuracies achievable with GPS observations are limited by many factors, such as satellite and receiver oscillator instabilities, and atmospheric modeling errors. The most significant factor limiting present results to approximately 1 ppm is, however, the affect of orbit errors. The existence of errors in the broadcast GPS ephemerides causes errors and discrepancies in the ground coordinate and coordinate difference solutions, and these discrepancies are apparent in results published to date [ie. Beutler et al., 1984; Beck et al., 1984; Goad and Remondi, 1984]. The uncertainty introduced into a baseline estimate due to orbital errors can be approximated by

$$db = b \frac{d\rho}{\rho} \tag{1.1}$$

where

- db is the baseline error,
- b is the baseline length,
- $d\rho$ is the orbit error, and
- ρ is the topocentric range from station to satellite.

This expression is a geometrical approximation and does not take into account the baseline and satellite pass orientation, however, it does provide a conservative estimate [Buffett,in prep.] which is useful for further discussions.

Based on the approximation given in Equation 1.1 and results published to date [ie. Bock et al.,1985], the broadcast ephemeris orbit error would be, on average, about 20 m and could be as high as 50 m . This level of orbit error is realistic for the broadcast orbit, and is within design specifications of the GPS Master Control Segment [Varnum and Chaffee,1982]. Accepting that GPS broadcast orbits are only accurate to 20 m, and precise post-mission ephemerides available to qualified users are accurate to approximately 10 m [Goad,personal communication,1984], Equation 1.1 shows that the achievable accuracy on a 1000 km baseline is 1 to 2 ppm. Equation 1.1 also shows that to achieve 0.1 ppm relative accuracies on such a baseline, the satellite orbit error can be no larger than 2.5 m . The requirement of satellite positions to an accuracy of 2.5 m creates the need for orbit improvement. Further, if the available satellite ephemerides are further degraded for civilian use, the need for orbit improvement will become more important.

The technique of orbit improvement is implemented by first representing a satellite pass with six reference initial conditions, obtainable from either the broadcast ephemeris or precise ephemeris file. A Keplerian representation was used for the initial conditions, however, it should be noted that this choice is not unique. Observations are required to the satellite pass from accurately positioned tracking stations. These observations can then be used in a least squares adjustment to solve for corrections to the satellite initial conditions, in effect improving the accuracy of computed satellite positions.

1.3 Description Of Present Study

The major objective of this research is to develop a prototype adjustment software package that will simultaneously process observations from multiple satellites and stations. The formulation is to incorporate full a priori estimates and weighting of station coordinates and satellite initial conditions. This aspect of the formulation allows for orbit improvement capabilities along with estimation of ground station coordinates and nuisance parameters.

The first step in this study, described in Chapter 2, involves an examination of the observations to be used. The observations available from GPS satellites that have been considered are pseudorange, Doppler, and single difference phase. The mathematical model for each observation type is given, with definitions of specific parameters pertaining to each.

The second phase of the study is the derivation of the adjustment model. The general form of the models used are given, then the linearized form of the partitioned adjustment equations are derived. This derivation, along with a brief overview on the computer programming of the adjustment, is given in Chapter 3.

The requirements of a tracking station network for orbit improvement are addressed in Chapter 4. The network configurations analyzed are given, and a discussion is presented on the required accuracy of the station coordinates. The approach taken to simulate orbit improvement tests and tracking network design is also given.

Simulated orbit improvement results are presented in Chapter 5. The results for each observation type are given and compared, along with test results for the separation of timing errors from orbit errors. The results for two tracking network configurations are also compared.

In Chapter 6 the results of station coordination are given. These results show a comparison of results for a typical broadcast orbit accuracy versus accuracies obtained after orbit improvement.

Finally, conclusions are drawn from the results of this study, and recommendations are made for additional future analysis.

CHAPTER 2

GPS OBSERVATIONS

2.1 Description Of Observation Types

The GPS satellite system provides two fundamental observation types, pseudorange measurements derived from a code modulated on the carrier signal, and phase measurements obtained from monitoring the incoming carrier signal. The pseudorange measurements are an important advantage of GPS over previous satellite systems, since they allow for instantaneous position computations when four satellites are observed simultaneously. The GPS satellites broadcast on two L band frequencies, 1575.42 MHz and 1227.6 MHz, called L1 and L2, respectively. Measurements on these two frequencies allow for the computation of a first order ionospheric correction. The L1 and L2 frequencies are also called precision (P) and coarse acquisition (C/A) codes, and a thorough description of these signals can be found in Spilker [1978]. The accuracy of pseudorange measurements on L1 and L2 are on the order of 4 m and 10 m, respectively [Martin,1978]. This level of observational accuracy is adequate for certain applications, such as navigation, however, more precise measurements are required to obtain precise geodetic results.

Carrier phase measurements have an accuracy of approximately 0.1 m [Martin,1978], providing the necessary precision for geodetic work. There are many measurement types associated with carrier phase observations, however, the various types basically arise from the method used for processing or differencing the phases. The results of Anderle [1982] were obtained treating phase observations in the conventional intermittently integrated Doppler approach. In this approach the instantaneous phases from one satellite are differenced with a reference frequency generated at one station receiver, producing Doppler beats which are counted over individual time intervals. If Doppler measurements are made with respect to an initial lock-on time, they can be processed as range differences. This method is known as continuously integrated Doppler (CID) and was used by Brown [1970]. The geometry of this observation type is shown pictorially in Figure 2.1a .

The phases at one epoch from a single satellite can be differenced across two stations, producing the observation type called single differences (SD) [Remondi, 1984; Delikaraoglou, 1985], shown in Figure 2.1b . Single differences that have been made at two stations to two different satellites at the same epoch in time can then be differenced, as shown in Figure 2.1c, producing double differences (DD). Finally, double differences from the same pairs of stations and satellites can be differenced in time, forming triple differences (TD), shown in Figure 2.1d .

A detailed description of SD, DD, and TD observation types is given in Remondi [1984]. Results using these three types are given in Goad and Remondi [1984], and in Remondi [1984]. The next three sections of this chapter outline the mathematical formulation for pseudorange, continuously integrated Doppler, and single difference phase observations. The formulations include specific nuisance parameters and systematic corrections pertaining to each observation type. The double and triple difference observation types have not been included in the program. The reason they are not included is that these differences are formed to cancel systematic effects, such as receiver and satellite clock error, and these effects have been explicitly modeled in the single difference observation equation. The further differencing of SD observations also results in a canceling of common orbit error, to a large degree. This result makes DD and TD observations useful for station coordination over relatively short lines, possibly up to a few hundred kilometres . The canceling effect, however, is undesirable when orbit improvement is carried out, since the observation becomes less sensitive to the orbit error that is being solved.

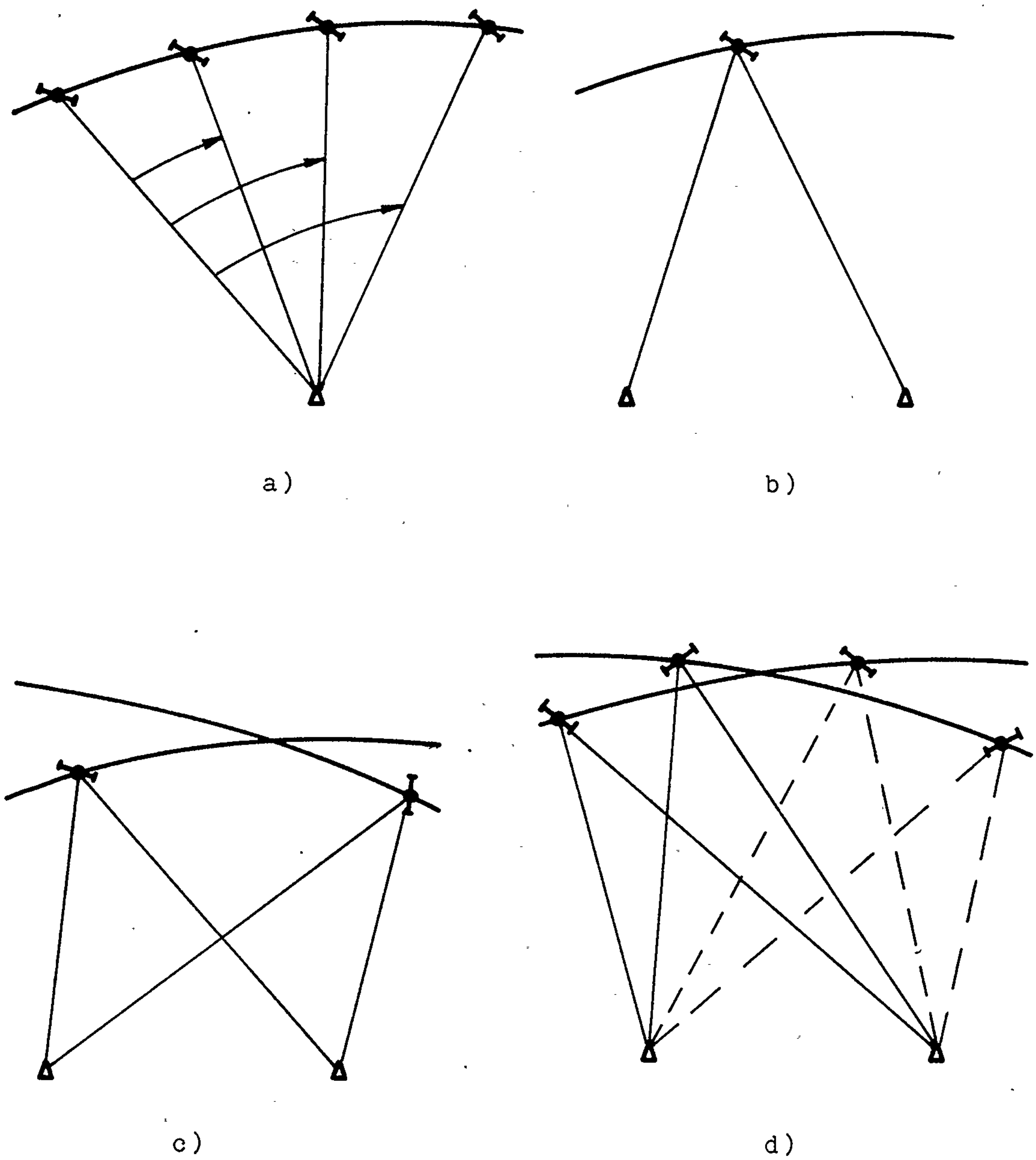

Figure 2.1: Geometry of Differenced Observations

a) Continuously Integrated Doppler b) Single Difference

c) Double Difference d) Triple Difference

2.2 Pseudorange Observations

The pseudorange observation equation involves one receiving station i and one satellite position j. The basic equation, neglecting atmospheric delays and timing errors, is written as:

$$\rho_{ij} = | r_j(t_j) - R_i | , \tag{2.1}$$

where

- ρ_{ij} is the topocentric range from receiver to satellite,
- $r_j(t_j)$ is the satellite position vector at satellite time t_j, and
- R_i is the station position vector.

The satellite and station position vectors are defined in terms of earth-fixed, geocentric-Cartesian coordinates as:

$$r_j(t_j) = [x_j'(t_j),\ y_j'(t_j),\ z_j'(t_j)]^t \tag{2.2}$$

and

$$R_i = [x_i, y_i, z_i]^t , \tag{2.3}$$

where

- $x_j'(t_j), y_j'(t_j), z_j'(t_j)$ are the satellite coordinates at satellite time t_j,
- x_i, y_i, z_i are the station coordinates, and
- $[\ ]^t$ indicates the transpose of a vector or matrix.

Atmospheric refraction has a delaying effect on pseudorange (and phase) observations, and must be included in Equation 2.1 . The Hopfield [1971] model has been used extensively in satellite applications to correct for the tropospheric refraction error. The correction is computed using surface measurements of temperature, pressure and relative humidity as follows:

$$\delta\rho_{trop} = \frac{K_d}{\sqrt{\sin(E^2+6.25)}} + \frac{K_w}{\sqrt{\sin(E^2+2.25)}} \qquad (2.4)$$

and

$$K_d = (1.552\text{x}10^{-5})PT^{-1}(148.72T-488.3552-h) \qquad (2.5)$$

$$K_w = (7.46512\text{x}10^{-5})eT^{-2}(11000-h) \qquad (2.6)$$

$$e = (0.01H)\exp(-37.2465+0.213166T-0.000256908T^2), \qquad (2.7)$$

where

$\delta\rho_{trop}$ is the tropospheric refraction correction,

T is the temperature in degrees Kelvin,

E is the elevation angle of the satellite in degrees,

P is the pressure in mbar,

e is the water vapour pressure in mbar,

H is the relative humidity in percent,and

h is the station orthometric height.

This tropospheric model is generally accepted to be accurate to approximately five percent of the total refraction effect, with the principal error source being in the wet component of the correction. A method used to account for this effect was adopted by Fell [1980], where a scaling parameter, C_r, is treated as a weighted parameter to be solved for in the adjustment. The use of water vapour radiometer measurements for precise tropospheric delay corrections would likely eliminate the need for C_r.

The upper portion of the atmosphere, known as the ionosphere, also affects pseudorange (and phase) measurements. There are two alternatives to making ionospheric corrections, depending upon how the observations were made. If measurements were made on one frequency only, a single frequency correction model can be used. The ionospheric corrections for this procedure are broadcast in the GPS satellite message, however, results to date have been worse when using this correction as compared to neglecting it [Beck et al., 1984; Lachapelle and Cannon, 1985]. Further research is being carried out for improving this one frequency model [Van Dierendonck, 1978]. The second method for correcting ionospheric delays can be used when measurements are made on the two broadcast frequencies, L1 and L2. Since the ionospheric delay is inversely proportional to frequency, a first order ionospheric correction can be computed as follows:

$$\delta\rho_{ion} = (\tilde{\rho}_1 - \tilde{\rho}_2)\,\frac{f_2^2}{f_2^2 - f_1^2}\ , \qquad (2.8)$$

where

$\delta\rho_{ion}$ is the ionospheric correction to the L1 pseudorange,

$\tilde{\rho}_i$ i=1,2 are the measured L1 and L2 pseudoranges respectively ,and

f_i i=1,2 are the L1 and L2 frequencies, respectively.

The studies done by Fell [1980] indicate an upper bound of approximately 5 mm on the residual error when using Equation 2.8 to correct for ionospheric delays. A residual ionospheric error or scaling parameter was not included since this modeling error is negligible.

The pseudorange (and phase) measurements are also affected by timing errors, both in the receiver and satellite clocks. Figure 2.2 shows the relationship between the various time scales involved. The GPS Master Control Station (MCS) establishes a master reference time scale, and the satellite oscillators are offset and drifting relative to this scale. The clock behaviour is monitored by the MCS and their states are estimated concurrently with the satellite ephemerides. The clock error is modeled by a second-order polynomial as follows:

$$\delta t_j = a_0 + a_1(t_j - t_o) + a_2(t_j - t_o)^2 , \qquad (2.9)$$

where

δt_j is the satellite clock error at time t_j,

t_o is the satellite clock reference time, and

a_0, a_1, a_2 are the clock model coefficients, broadcast in the satellite message.

Applying the correction δt_j to t_j brings the satellite time approximately into alignment with the master reference time scale. The above clock model was used in the adjustment formulation, with the broadcast coefficients a_0, a_1 and a_2 treated as weighted parameters in order to improve their values in the adjustment process.

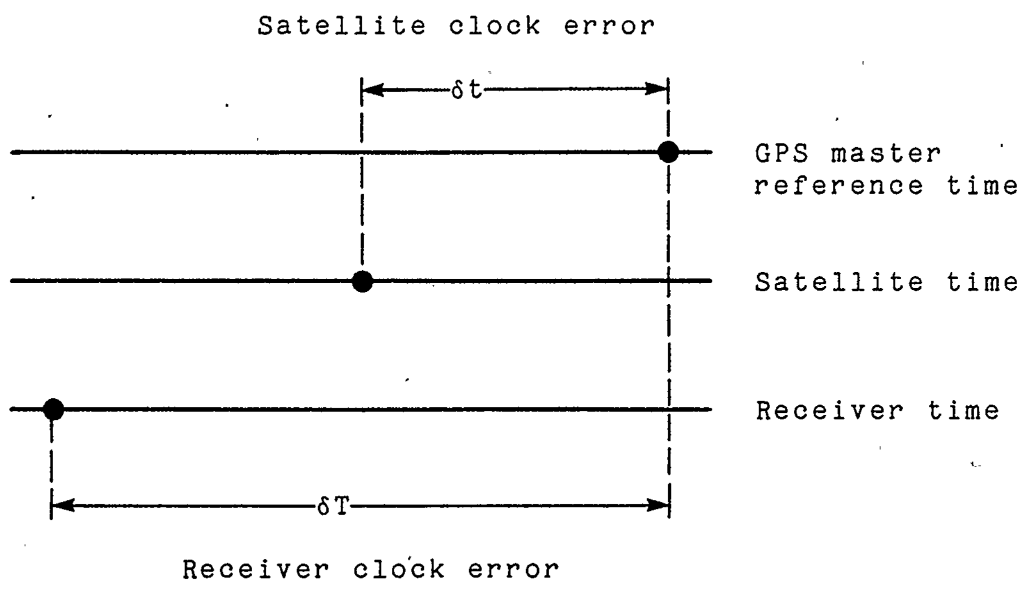

Figure 2.2: GPS Time Scales

The receiver clock is also offset and drifting relative to the master time scale, and the error model used has the same form as Equation 2.9. The formulation used is

$$\delta T_i = A_0+A_1(T_i-T_o)+A_2(T_i-T_o)^2 , \qquad (2.10)$$

where

δT_i is the receiver clock error at time T_i,

T_o is the receiver clock reference time, and

A_0, A_1, A_2 are the receiver clock model coefficients.

The receiver clock coefficients are also treated as weighted parameters in the adjustment formulation, so that a priori estimates may be used properly.

The final pseudorange observation equation, including atmospheric and timing corrections, is given in Equation 2.11.

$$\tilde{\rho}_{ij} = | r_j(t_j)-R_i |+\delta \rho_{ion}+\delta \rho_{trop}(1+C_r)+c\delta t_j-c\delta T_i , \qquad (2.11)$$

where

$\tilde{\rho}_{ij}$ is the observed pseudorange, and

c is the velocity of light.

2.3 Doppler Observations

The Doppler observation equation involves one receiving station i and two satellite positions j and k.

A detailed derivation of the Doppler equation can be found in many references, where the specialized form for continuously integrated measurements is also given [eg. Brown,1970; Wells,1974]. Neglecting atmospheric and timing effects, the basic equation is written as:

$$N_{ijk} = (f_g-f_s)\Delta T_{kj}+f_s c^{-1}\Delta\rho_{ijk} , \qquad (2.12)$$

where

N_{ijk} is the Doppler count,

f_g is the receiver generated reference frequency,

f_s is the satellite carrier frequency,

$\Delta T_{kj} = T_k-T_j$ is the time interval determined from the receiver oscillator, and

$\Delta\rho_{ijk} = | r_k(t_k)-R_i |-| r_j(t_j)-R_i |$

is the range difference from ground station i between satellite positions j and k. The Doppler equation is analogous to a measurement of the difference in range at two epochs in time. The tropospheric delay correction can therefore be computed as the difference of two pseudorange corrections, as follows:

$$\Delta\rho_{trop} = \delta\rho^k_{trop}-\delta\rho^j_{trop} , \qquad (2.13)$$

where

$\Delta\rho_{trop}$ is the Doppler tropospheric correction,and

$\delta\rho^k_{trop}$,$\delta\rho^j_{trop}$ are the range tropospheric corrections computed using Equation 2.4 .

It should be noted that this correction is in metres and must be scaled into cycles to be applied to Equation 2.12.

The ionospheric delay for Doppler measurements can be computed from observations on the two carrier frequencies. The correction, given in Equation 2.14, was developed using the same procedure found in Krakiwsky and Wells [1971] for Transit Doppler observations, except the GPS L1 and L2 frequencies were used. In equation form,

$$\Delta N_1 = \frac{36}{23.29} \left| \frac{77}{60} \tilde{N}_2 - \tilde{N}_1 \right| , \qquad (2.14)$$

where

ΔN_1 is the L1 ionospheric correction, and

$\tilde{N}_i$ $i=1,2$ are the observed L1 and L2 Doppler counts, respectively.

The time interval ΔT_{kj} in Equation 2.12 is determined by the receiver oscillator, and therefore errors in the receiver frequency will affect the observations. The time offset A_0 in Equation 2.10 will cancel since it is constant over the interval. The remaining errors of time drift A_1 and ageing rate A_2 are equivalent to a frequency offset and frequency drift respectively [Davidson et al.,1983], as shown below :

$$A_1 = \frac{\Delta f_o}{f_g} \quad , \quad A_2 = \frac{\dot{f}}{2f_g} \tag{2.15}$$

where

A_1, A_2 are the time drift and ageing coefficients defined in Equation 2.10,

$\Delta f_o, \dot{f}$ are the frequency offset and drift respectively, and

f_g is the nominal oscillator frequency.

The correction for the receiver oscillator can now be computed in terms of frequency as follows :

$$\begin{aligned} \Delta f_k &= \Delta f_o + \dot{f}\Delta T_{kj} \\ &= A_1 f_g + 2A_2 f_g \Delta T_{kj} \ , \end{aligned} \tag{2.16}$$

where

Δf_k is the frequency offset at time T_k, and

$\Delta T_{kj} = T_k - T_j$ is the receiver time interval.

It should be noted that this offset is in Hertz, and must be scaled by the time interval ΔT_{kj} to be applied to Equation 2.12 . The final equation for continuously integrated Doppler measurements is given below. The satellite position subscript j has been replaced by subscript o, indicating the measurement N_{ijk} and corresponding time interval ΔT_{kj} are with respect to the initial lock-on time T_o. This formulation makes it necessary to solve for an additional unknown parameter r_o, the range bias at lock-on time, namely :

$$\tilde{N}_{iok} = (f_g - f_1)\Delta T_{ko} + \Delta T_{ko}(A_1 f_g + 2A_2 f_g \Delta T_{ko}) + f_1 c^{-1} \Delta\rho_{iok} \quad (2.17)$$

and

$$\Delta\rho_{iok} = | r_k(t_k) - R_i | - r_o + f_1 c^{-1}(1+C_r)\Delta\rho_{trop} + \Delta N_1 \,, \quad (2.18)$$

where

$\tilde{N}_{iok}$ is the observed Doppler count, on the L1 frequency, at time T_k since reference time T_o,

$\Delta T_{ko} = T_k - T_o$ is the receiver time interval since lock-on time T_o, and

r_o is the range bias at lock-on time.

The above Doppler formulation is given in terms of f_1, the L1 satellite frequency, since the ionospheric correction has been developed to give the correct value for L1 observations. However, observations are required on both the L1 and L2 frequencies so that this correction can be computed.

2.4 Single Difference Phase Observations

Phase observations, denoted by ϕ, are produced by determining the difference between the phase of a satellite generated signal ϕ_S and the phase of a receiver generated reference signal ϕ_R. For an arbitrary epoch i, the satellite signal is transmitted at satellite time t_i and received at receiver time T_i. The instantaneous phase

ϕ_j, involving one satellite position and one ground station j, is defined as follows:

$$\begin{aligned}\phi_j &= \phi_S(t_i)-\varphi_R(T_i)\\ &= \phi_S(T_i-\rho_j c^{-1})-\varphi_R(T_i)\ ,\end{aligned} \tag{2.19}$$

where

ρ_j is the receiver to satellite slant range.

Note that in Equation 2.19 the effect of atmospheric delays and timing errors have been neglected, and that the satellite phase ϕ_s is defined in terms of the receipt time T_i minus the propagation time $\rho_j c^{-1}$. Goad and Remondi [1984] have indicated that, since the oscillators involved are quite stable over short periods of time, the first term in Equation 2.19 can be adequately approximated by a linear Taylor series expansion of the form

$$\phi(T+\Delta T) = \phi(T)+f_s\Delta T\ , \tag{2.20}$$

where f_s is the oscillator frequency.

Substituting (2.20) into (2.19) yields

$$\phi_j = \phi_S(T_i)-f_S\rho_j c^{-1}-\phi_R(T_i)+N_j \tag{2.21}$$

where N_j is an unknown ambiguity parameter.

The parameter N_j compensates for the fact that the first term in Equation 2.21 is less than one cycle, and the second term contains many cycles.

The single difference phase observable used in this research involves a single satellite position and two ground stations j and k. The observation is formed by simply differencing the measurements, represented by Equation 2.21, taken at two stations. The resulting equation has the following form:

$$\Delta\phi_{jk} = f_s c^{-1}(\rho_j - \rho_k) - (\phi_{R_k} - \phi_{R_j}) + (N_k - N_j) \quad , \qquad (2.22)$$

where the first term is the difference of slant ranges between one satellite position and the two receiving stations j and k; the second term is the phase difference between the two station clocks; and the third term is the difference of two station/satellite dependant unknown ambiguity parameters.

The tropospheric and ionospheric delay corrections are applied to single difference phase observations in the same manner as for Doppler measurements, given in Equations 2.13 and 2.14 respectively. The phase difference between the two station clocks is corrected for oscillator instabilities in a similar manner to Equation 2.10 for pseudorange measurements, except the correction involves the difference of two different station clock corrections. The final single difference phase observation equation is given as follows:

$$\Delta\tilde{\phi}^{1}_{jk} = f_1 c^{-1}(\rho_j - \rho_k) + \Delta\phi_{ion} + \Delta\varphi_{trop} + \Delta\varphi_{time} + N_k - N_j \quad , \qquad (2.23)$$

and

$$\Delta\phi_{ion} = \frac{36}{23.29} \left| \frac{77}{60} \Delta\tilde{\phi}^2_{jk} - \Delta\tilde{\phi}^1_{jk} \right| \tag{2.24}$$

$$\Delta\phi_{trop} = f_1 c^{-1}(\delta\rho^k_{trop} - \delta\rho^j_{trop})(1+C_r) \tag{2.25}$$

$$\Delta\phi_{time} = f_1(\Delta A_0 - \Delta A_1 \Delta T - \Delta A_2 \Delta T^2) \tag{2.26}$$

$$\rho_k - \rho_j = | r_i(t_i) - R_k | - | r_i(t_i) - R_j | , \tag{2.27}$$

where

$\Delta\tilde{\phi}^i_{jk}$ $i=1,2$ are the observed phase differences, on L1 and L2 frequencies respectively, between stations j and k and a single satellite position,

$\Delta\phi_{ion}$ is the ionospheric correction for L1 observations,

$\Delta\phi_{trop}$ is the tropospheric correction,

$\delta\rho^j_{trop}$, $\delta\rho^k_{trop}$ are the individual tropospheric corrections computed using Equation 2.4 based on ranges to stations j and k respectively,

$\Delta\phi_{time}$ is the correction between receiver clocks ,

$\Delta A_i = A^k_i - A^j_i$ $i=0,2$ are the differences in clock model coefficients A_0, A_1, and A_2 for stations j and k, and

$\Delta T = T_i - T_o$ is the receiver observation time T_i minus the receiver clock model reference time T_o .

The single difference phase measurement defined in Equation 2.23 is for observations on the L1 frequency, as denoted by the superscript 1 in the term $\Delta\tilde{\phi}^1_{jk}$. The reason this is specified is so the ionospheric correction term $\Delta\phi_{ion}$ has the correct value. However, it should be noted that measurements are necessary on both the L1 and L2 frequencies in order for this correction to be computed.

In the adjustment formulation, the unknown ambiguity parameters are not treated in the usual manner, where each baseline has a parameter associated with it for each satellite pass. Since a multi-station approach is used, this method would produce dependant ambiguity parameters when observations from three or more stations are processed simultaneously. The method used establishes a master station within the network of observing stations. There will then be an ambiguity parameter for every other station in the network, relative to the master station, for each satellite pass observed.

CHAPTER 3

ADJUSTMENT FORMULATION

The three observation equations given in Chapter 2 relate the observations to particular constants, such as the velocity of light, and to the unknown parameters to be solved for. The measurement of more observations than unknowns results in a redundant set of equations, which increases the accuracy of the solution and yields the ability to do statistical testing. The following sections of this chapter give the mathematical models used to solve this set of redundant equations using the method of least squares. The method involves linearizing the model using a Taylor series expansion, then deriving the adjustment equations via the Lagrange method and matrix partitioning techniques [see Vanicek and Krakiwsky, 1982]. The last section in this chapter gives a brief overview on the computer coding of the adjustment equations.

3.1 Estimation Model

The vector of observations used in the adjustment is denoted by ℓ. The three observation types are processed independantly in the prototype program, with an option available for combining solutions using a summation of normal equations technique. The unknown parameters have been partitioned into three sets:

1) The first set contains all tracking station Cartesian coordinates $[x_i, y_i, z_i]$, and is denoted by x.
2) The second set is comprised of six Keplerian reference initial conditions $[a_o, e_o, \omega_o, i_o, \Omega_o, M_o]$ for each satellite pass, and is denoted by z_o.
3) The last set contains the following nuisance parameters defined in Chapter 2:
   i) scale parameter C_r to resolve unaccounted for tropospheric refraction;
   ii) corrections to satellite clock polynomial coefficients (a_0, a_1, a_2);
   iii) receiver clock model coefficients (A_0, A_1, A_2);
   iv) a range bias at lock-on time for each station/satellite combination (r_o, for Doppler only);
   v) an ambiguity parameter for each station/satellite combination relative to a master station (N_i, for single difference phase only); and

vi) an unknown scale factor to account for solar radiation pressure in the force model.

The third set of unknown parameters is included in vector x in the current prototype adjustment program. A future version may have this set explicitly partitioned, and possibly divided into pass dependant and station dependant parameters.

Information on the accuracy of observations is input into the estimation model via covariance matrix C_ℓ. Options allow for a priori estimates of x and z_o to be input, along with their associated covariance matrices C_x and C_{z_o}.

The estimation model used is comprised of two functions, f_1 and f_2, given below:

$$f_1(x, x', \ell) = 0 \quad , C_x, C_\ell \tag{3.1}$$

$$f_2(x'+s, z_o) = 0 \quad , C_s, C_{z_o} \tag{3.2}$$

where

x' is the vector of satellite cartesian coordinates, and

s is the signal component.

The first function, f_1, corresponds to a pure geometric mode of satellite positioning [Schwarz, 1969], relating ground station and satellite Cartesian coordinates to the vector of observations. The second function defines the relationship between the satellite initial conditions and the satellite Cartesian coordinates at an arbitrary epoch. This relationship involves a solution of the equations of motion for the satellite in terms of the initial conditions.

The superiority of a short-arc state vector approach for solving corrections to satellite initial conditions over an orbit bias approach is shown conceptually in Figure 3.1 . In the orbit bias approach, generally three biases in the along-track, radial, and out-of-plane directions are solved for. This method affords some improvement in the satellite positions, however, the estimated orbit will not accurately follow the 'true' orbit since the biases cannot vary in time. Using the short-arc state vector approach, the shape of the orbit should be accurately defined by the force model and perturbation equations used. The solution provides corrections to the initial conditions which, when added to the nominal values, yield an accurate estimated orbit that closely follows the 'true' orbit.

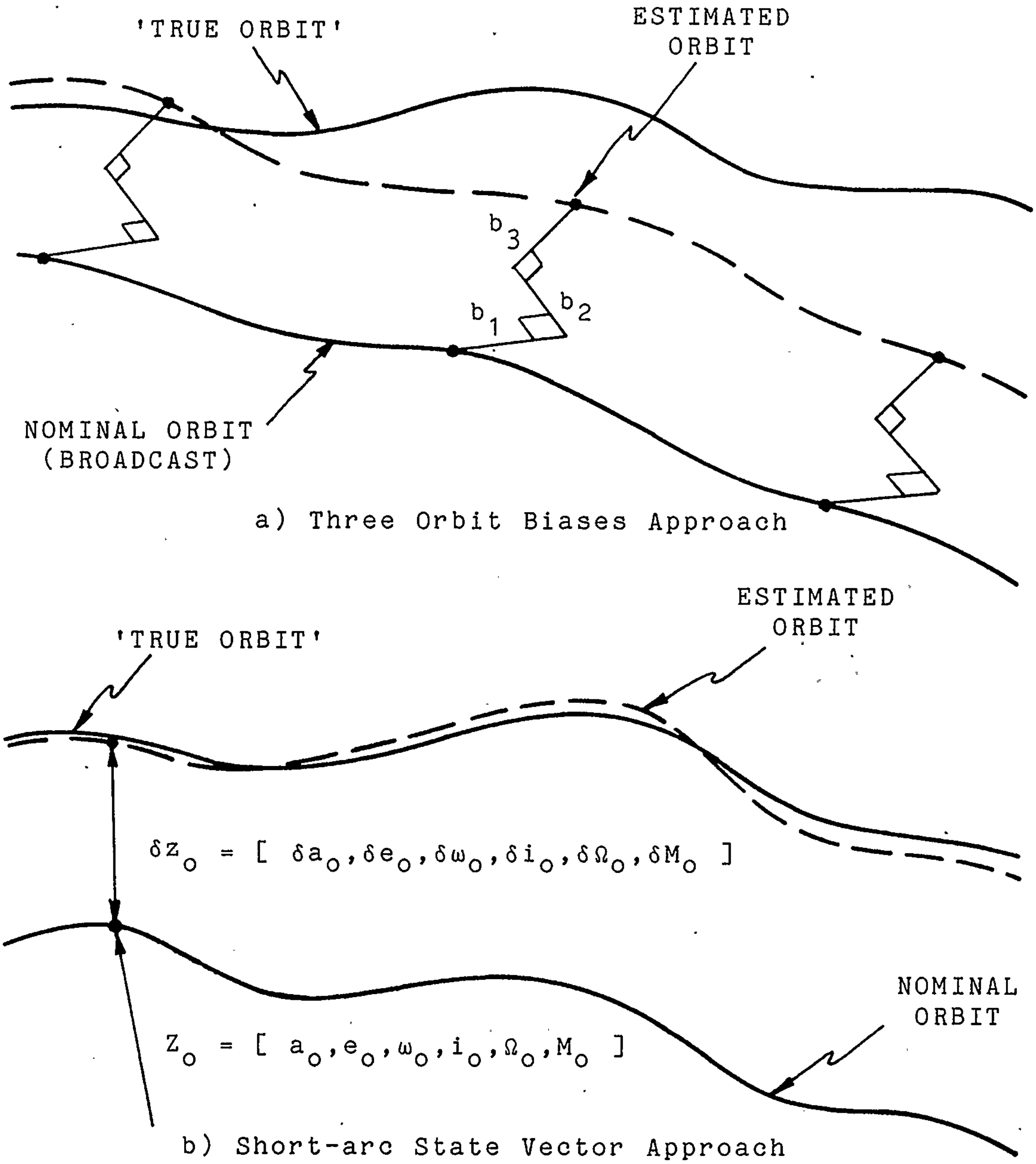

Figure 3.1: Approaches to Orbit Improvement

Note that in Equation 3.2, the provision to treat f_2 as imperfect has been incorporated, and the imperfection has been treated as a signal s. To utilize this aspect of the formulation an a priori signal covariance matrix C_s is required. This signal covariance matrix may be determined by analyzing the higher order perturbations truncated from the force model used. Another possible source for obtaining C_s may be from an analysis of the observation residuals after an orbit improvement solution.

The solution of the equations of motion for GPS satellites was analyzed and programmed by Bruce Buffett [Buffett, in prep.]. Some comments on certain aspects of this solution will be given in section 3.3 .

The linearized form of f_1 is

$$A_x \delta x + A_{x'} \delta x' + w = r \tag{3.3}$$

where

$$A_x = \frac{\partial f_1}{\partial x} ,$$

$$A_{x'} = \frac{\partial f_1}{\partial x'} ,$$

$$w = f_1(x^0, x'^0, \ell)$$

and δx, $\delta x'$ and r are corrections to the approximate values of the unknowns x^0 and x'^0, and the observations ℓ, respectively.

The linearized form of the second function, f_2, is

$$\delta x' = B\delta z_o - s \tag{3.4}$$

where

$$B = B_1 B_2$$

$$= \frac{\partial x'(t)}{\partial z(t)} \frac{\partial z(t)}{\partial z_o} \tag{3.5}$$

Equation 3.4 relates corrections to the satellite initial conditions, δz_o, to corrections to satellite Cartesian coordinates $\delta x'$, at an arbitrary epoch t.

The covariance matrix of the signal, C_s, can be defined as follows:

$$C_s = B_1 C_{\delta z} B_1^t \tag{3.6}$$

where $C_{\delta z}$ is the a priori signal covariance matrix for the Keplerian orbital elements.

The combined estimation model is formed by explicitly substituting Equation 3.4 into Equation 3.3, yielding

$$A_x \delta x + A_{x'}(B\delta z_o - s) + w = r \tag{3.7}$$

or equivalently,

$$A_x \delta x + A_{x'} B\delta z_o - A_{x'} s + w = r \tag{3.8}$$

with a priori covariance matrices C_x, C_{z_o}, C_s and C_ℓ. The model of Equation 3.8 is in the category of least squares collocation [Schwarz 1976 ; Moritz 1972], and the formulation can be transformed into hypermatrix notation as shown below. Equation 3.8 can be rewritten as

$$[\, A_x \quad A_{x'}, B \,] \begin{bmatrix} \delta x \\ \delta z_o \end{bmatrix} + [\, -A_{x'} \,]\, s + w = r \quad . \tag{3.9}$$

The hypermatrices are then defined as follows:

$$A^* = [\, A_x \quad A_{x'}, B \,] \quad , \tag{3.10}$$

$$x^* = [\, \delta x \quad \delta z_o \,]^t \quad , \tag{3.11}$$

$$B^* = [\, -A_{x'} \,] \quad . \tag{3.12}$$

The above equations can then be rewritten in collocation form as

$$A^* x^* + B^* s + w = r \quad , \tag{3.13}$$

with corresponding covariance matrices

$$C_{x^*} = \begin{bmatrix} C_x & 0 \\ 0 & C_{z_o} \end{bmatrix} , \; C_s , \; C_\ell \; . \tag{3.14}$$

3.2 Least Squares Solution

The least squares solution to the above mathematical extremum problem can be found using the Lagrange method. In this method, the problem is defined in terms of a variation function, ϕ, where a vector of Lagrange multipliers k are introduced as follows:

$$\phi = r^t C_\ell^{-1} r + x^{*t} C_{x^*}^{-1} x^* + s^t C_s^{-1} s + 2k^t (A^* x^* + B^* s + w - r) \quad . \tag{3.15}$$

The desired least squares solution is found by minimizing the variation function of Equation 3.15 . This is accomplished by taking the partial derivatives of ϕ with respect to the unknowns r, x^*, s and k , then setting these derivatives equal to zero and solving the resulting set of equations, given in Equations 3.16 to 3.19 .

$$\frac{\partial \phi}{\partial r} = C_\ell^{-1} r - k = 0 \quad , \tag{3.16}$$

$$\frac{\partial \phi}{\partial x^*} = C_{x^*}^{-1} x^* + A^{*t} k = 0 \quad , \tag{3.17}$$

$$\frac{\partial \phi}{\partial s} = C_s^{-1} s + B^{*t} k = 0 \quad , \tag{3.18}$$

$$\frac{\partial \phi}{\partial k} = A^* x^* + B^* s + w - r = 0 \quad . \tag{3.19}$$

The solution of this set of equations is a minimum if the second derivatives are positive or zero. This is confirmed , since the second derivatives of Equations 3.16 to 3.18 are equal to C_ℓ^{-1}, $C_{x^*}^{-1}$ and C_s^{-1} respectively, and covariance matrices are positive definite by definition, and the second derivative of equation 3.19 is equal to zero.

The most expanded form of the least squares normal equations pertaining to Equations 3.16 to 3.19 is

$$\begin{bmatrix} C_\ell^{-1} & -I & 0 & 0 \\ -I & 0 & A^* & B^* \\ 0 & A^{*t} & C_x^{-1*} & 0 \\ 0 & B^{*t} & 0 & C_s^{-1} \end{bmatrix} \begin{bmatrix} r \\ k \\ x^* \\ s \end{bmatrix} + \begin{bmatrix} 0 \\ w \\ 0 \\ 0 \end{bmatrix} = \begin{bmatrix} 0 \\ 0 \\ 0 \\ 0 \end{bmatrix} \quad . \qquad (3.20)$$

This system of equations is reduced by first eliminating the vectors r and k using a special elimination technique [e.g. Thomson 1969 ; Wells and Krakiwsky 1971]. Applying the technique to Equation 3.20 twice yields

$$\begin{bmatrix} C_x^{-1*}+A^{*t}C_\ell^{-1}A^* & A^{*t}C_\ell^{-1}B^* \\ B^{*t}C_\ell^{-1}A^* & C_s^{-1}+B^{*t}C_\ell^{-1}B^* \end{bmatrix} \begin{bmatrix} x^* \\ s \end{bmatrix} +$$

$$\begin{bmatrix} A^{*t}C_\ell^{-1}w \\ B^{*t}C_\ell^{-1}w \end{bmatrix} = \begin{bmatrix} 0 \\ 0 \end{bmatrix} \quad . \qquad (3.21)$$

Row and column interchanges are now used in order to eliminate s, resulting in

$$\{C_x^{-1*}+A^{*t}C_\ell^{-1}A^*-A^{*t}C_\ell^{-1}B^*(C_s^{-1}+B^{*t}C_\ell^{-1}B^*)^{-1}B^{*t}C_\ell^{-1}A^*\}x^* \quad +$$

$$\{A^{*t}C_\ell^{-1}w-A^{*t}C_\ell^{-1}B^*(C_s^{-1}+B^{*t}C_\ell^{-1}B^*)^{-1}B^{*t}C_\ell^{-1}w\} = 0 \quad . \qquad (3.22)$$

The hypermatrix definitions given in Equations 3.10, 3.11, 3.12 and 3.14 can now be substituted into Equation 3.22, and the resulting system further partitioned to yield solutions for δx and δz_o as shown below.

$$\{C_x^{-1}+N_{11}-N_{33}-(N_{12}-N_{34})(C_{z_o}^{-1}+N_{22}-N_{44})^{-1}(N_{21}-N_{43})\}\delta x \quad +$$

$$\{U_1-U_3-(N_{12}-N_{34})(C_{z_o}^{-1}+N_{22}-N_{44})^{-1}(U_2-U_4)\} = 0 \qquad (3.23)$$

$$\{C_{z_o}^{-1}+N_{22}-N_{44}-(N_{21}-N_{43})(C_x^{-1}+N_{11}-N_{33})^{-1}(N_{12}-N_{34})\}\delta z_o +$$

$$\{U_2-U_4-(N_{21}-N_{43})(C_x^{-1}+N_{11}-N_{33})^{-1}(U_1-U_3)\} = 0 \quad , \qquad (3.24)$$

where

$$N_{11} = A_x^t C_\ell^{-1} A_x \ ,$$

$$N_{12} = A_x^t C_\ell^{-1} A_{x'} B \ ,$$

$$N_{21} = N_{12}^t = B^t A_{x'}^t C_\ell^{-1} A_x \ ,$$

$$N_{22} = B^t A_{x'}^t C_\ell^{-1} A_{x'} B \ ,$$

$$N_{33} = A_x^t C_\ell^{-1} A_{x'} D^{-1} A_{x'}^t C_\ell^{-1} A_x \ ,$$

$$N_{34} = A_x^t C_\ell^{-1} A_{x'} D^{-1} A_{x'}^t C_\ell^{-1} A_{x'} B \ ,$$

$$N_{43} = N_{34}^t = B^t A_{x'}^t C_\ell^{-1} A_{x'} D^{-1} A_{x'}^t C_\ell^{-1} A_x \ ,$$

$$N_{44} = B^t A_{x'}^t C_\ell^{-1} A_{x'} D^{-1} A_{x'}^t C_\ell^{-1} A_{x'} B \ ,$$

$$D = C_s^{-1} + A_{x'}^t C_\ell^{-1} A_{x'} \ ,$$

$$U_1 = A_x^t C_\ell^{-1} w \ ,$$

$$U_2 = B^t A_{x'}^t C_\ell^{-1} w \ ,$$

$$U_3 = A_x^t C_\ell^{-1} A_{x'} D^{-1} A_{x'}^t C_\ell^{-1} w \ , \text{ and}$$

$$U_4 = B^t A_{x'}^t C_\ell^{-1} A_{x'} D^{-1} A_{x'}^t C_\ell^{-1} w \ .$$

The signal component of the formulation is not incorporated in the present version of the prototype adjustment package. The corresponding equations are obtained by deleting all terms involving C_s, the a priori signal covariance matrix. The resulting equations, without the signal component, are

$$\{C_x^{-1}+N_{11}-N_{12}(C_{z_o}^{-1}+N_{22})^{-1}N_{21}\}\delta x + \{U_1-N_{12}(C_{z_o}^{-1}+N_{22})^{-1}U_2\} = 0 \tag{3.25}$$

and

$$\{C_{z_o}^{-1}+N_{22}-N_{21}(C_x^{-1}+N_{11})^{-1}N_{12}\}\delta z_o + \{U_2-N_{21}(C_x^{-1}+N_{11})^{-1}U_1\} = 0 \quad . \tag{3.26}$$

The estimated station Cartesian coordinates and nuisance parameters are computed as follows:

$$\hat{x} = x^o+\delta x \quad , \tag{3.27}$$

with covariance matrix

$$C_{\hat{x}} = \{C_x^{-1}+N_{11}-N_{12}(C_{z_o}^{-1}+N_{22})^{-1}N_{21}\}^{-1} \quad . \tag{3.28}$$

The estimated satellite initial conditions are given by

$$\hat{z}_o = z_o^o+\delta z_o \tag{3.29}$$

with covariance matrix

$$C_{\hat{z}_o} = \{C_{z_o}^{-1}+N_{22}-N_{21}(C_x^{-1}+N_{11})^{-1}N_{12}\}^{-1} \quad . \tag{3.30}$$

The ability to do orbit improvement has been incorporated in the least squares adjustment by treating the satellite initial conditions, z_o, as weighted parameters , with a priori covariance matrix C_{z_o}. In addition, a solar radiation pressure constant is also treated as a weighted parameter. The orbit improvement mode is obtained by increasing the a priori initial condition variances used in C_{z_o}. The ground station coordination mode is obtained by representing a precise orbit with small variances in C_{z_o}, and relaxing the station coordinate covariance matrix C_x or deleting it altogether. Simultaneous improvement of ground station coordinates and satellite initial conditions is also possible when both C_x and C_{z_o} are relaxed.

3.3 Adjustment Software

The adjustment software developed for GPS orbit improvement and precise positioning consists of two distinct program packages. The first, Adjustment Software for TRacking station and Orbit parameters (ASTRO), was developed by the author for the processing of observations, formation of the normal equations, iteration until the solution has converged, and computation and output of final results. The second program package, Program for Earth orbiting Geodetic Satellites (PEGS), was developed by Bruce Buffett [Buffett, in prep.] to compute satellite Cartesian coordinates using numerical integration of the equations of motion in terms of six Keplerian initial conditions. The GPS observations were simulated using program DIFGPS, developed at The University of New Brunswick [Davidson et al., 1983]. This program was modified by the author to compute satellite coordinates using PEGS, and to produce data files compatible with ASTRO.

The main program and 34 subroutines of ASTRO are all written in FORTRAN 77. The logic flow of program ASTRO is shown in Figure 3.2. The program starts by setting various constants and reading ground station, satellite and observation data files. Description of the data file formats are given in External Appendix I. The program then branches for the particular observation type being processed. For each type , partial derivatives are evaluated with satellite Cartesian coordinates computed via calls to PEGS. The observations are processed sequentially, using summation techniques to form the normal equation blocks given in section 3.2 . The sequential formation of normal equations reduces execution time and storage requirements, since large design matrices A_x and A_x, do not have to be stored or mathematically processed. The program execution, having returned to a single flow, then adds all a priori covariance information and computes a least squares solution. The corrections are added to approximate values and tested against convergence tolerances. If another iteration is required, the program re-processes all observations using updated values of the parameters. In the second and subsequent iterations, program PEGS is called with an option to enable analytical computations rather than numerical integration. The corrections to Keplerian initial conditions, δz_o, are passed to PEGS, which uses analytical techniques to compute corrections to satellite Cartesian coordinates, rather than re-integrating the orbit with updated Keplerian initial conditions. This procedure proved to be computationally efficient, however storage requirements are increased since satellite Cartesian coordinates must be retained in memory. Program PEGS also uses analytical formulations to evaluate the Jacobian matrices B_1 and B_2 . Once all corrections are below convergence tolerance, the solutions and associated covariance matrices are computed and printed out. There is also an option available for storing the normal equation matrices, which could later be used for combining independent solutions.

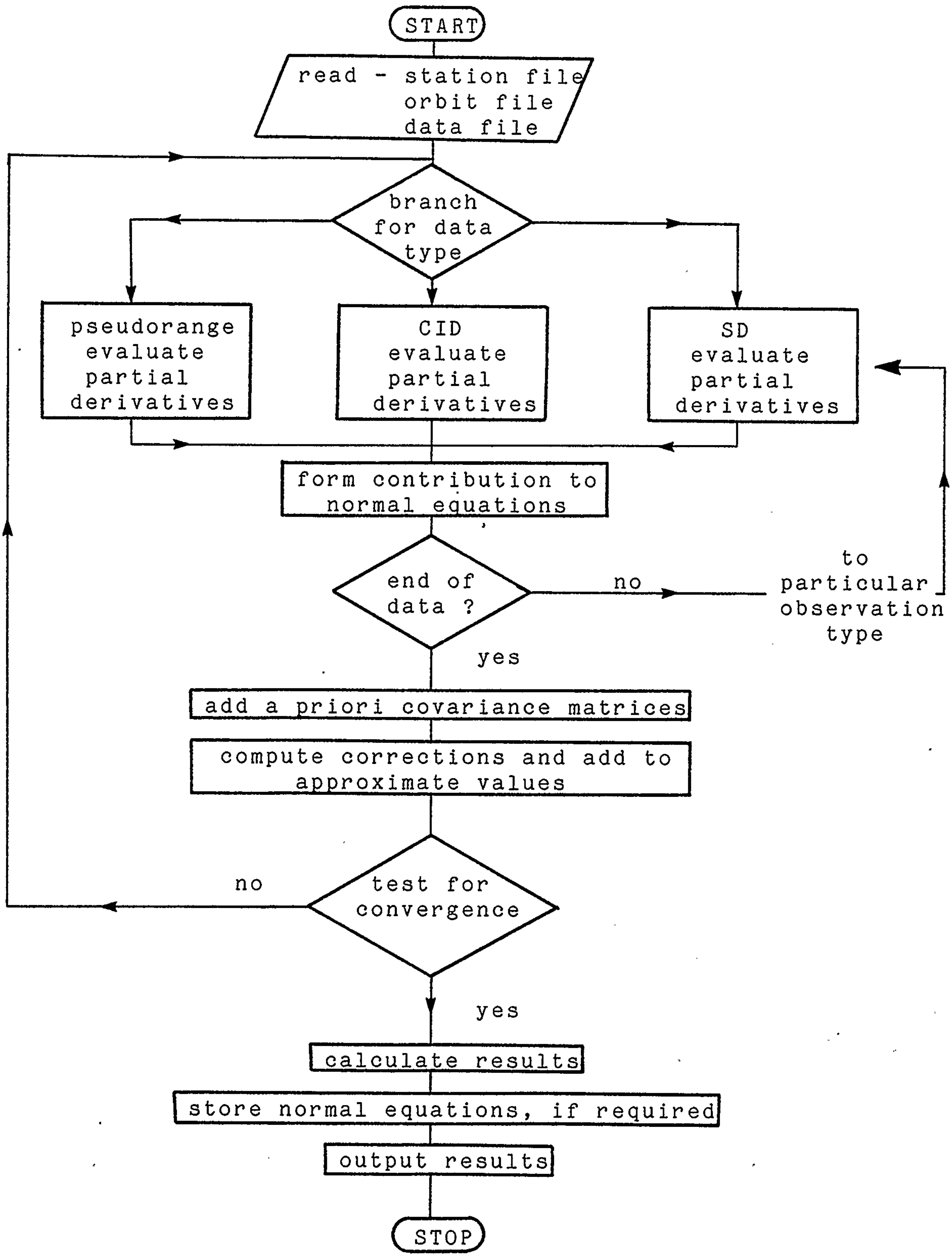

Figure 3.2: ASTRO Conceptual Flowchart

CHAPTER 4

TRACKING NETWORK DESIGN

The effect of satellite orbit errors on the accuracy of positioning results was represented in Chapter 1 by Equation 1.1 . This relationship shows that given the available accuracy of 20 to 50 m for GPS satellite ephemerides, the relative accuracy obtainable on baselines will be on the order of 1 ppm at best. Results for GPS positioning published to date have often reached this level of accuracy [e.g. Lachapelle et al.,1985 ; Goad and Remondi, 1984 ; Beck et al., 1984], and many researchers now believe the error limiting results to this level of accuracy is in the satellite orbit. To obtain baseline accuracies of 0.1 ppm, satellite positions will have to be known to an accuracy of 2.5 m .

The ability to resolve errors in the orbit elements defining a short-arc (four hour) GPS satellite pass is mainly dependant upon the tracking station geometry, the observation accuracy and the observation type [Nakiboglu et al., 1985]. The next section of this chapter gives an outline of the tracking network configurations used to study short-arc GPS orbit improvement over Canada. The criteria for selecting the two configurations are given, with a discussion on the accuracy requirements for tracking station coordinates and frequency standards. The following section outlines how GPS observations were simulated for this study. The final section in this chapter gives the procedures used for studying GPS orbit improvement capabilities over Canada. The methods used for comparing observation types, tracking network configurations, and sensitivity to different orbit elements are given. The solution of receiver clock errors is outlined, for both orbit improvement and station coordination tests. Finally, the approach used to compare results of station solutions using orbits with broadcast ephemeris accuracy versus improved orbits is outlined.

4.1 Tracking Network Configurations

The use of regional tracking networks to improve GPS orbit accuracy is being investigated by various research groups [Stolz et al.,1984 ; Davidson et al.,1985]. The concept of orbit improvement employed at The University of Calgary involves modeling all perturbing forces acting upon the satellites to a desired level of accuracy, in this case 2.5 m . Each satellite pass is defined using six reference initial conditions, and the equations of motion for the satellite under the adopted force model are either numerically integrated or analytically evaluated to generate satellite Cartesian coordinates [Nakiboglu et al.,1984]. The reference initial conditions used in this study are Keplerian orbital elements. A detailed description of the orbit modeling used in this study can be found in Buffett [in prep.]. The satellites are monitored from accurately positioned tracking stations in the region of interest, and using these observations corrections to the reference initial conditions are computed in a least squares adjustment.

The two tracking station configurations used in this study are shown in Figure 4.1, and the station coordinates are given in Table 4.1 .

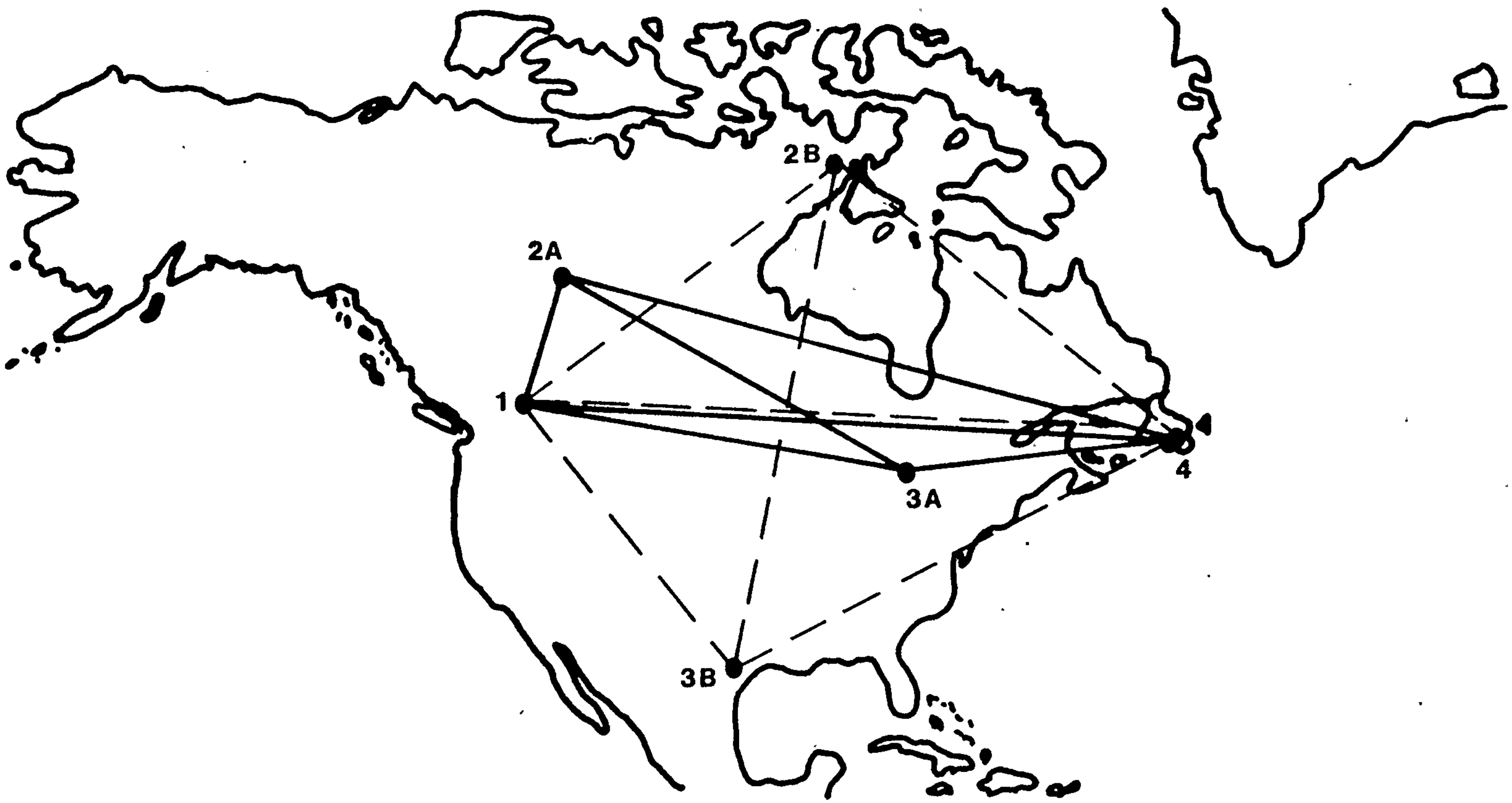

Figure 4.1: Tracking Network Configurations

Network A ———————— Stations 1, 2A, 3A, 4

Network B — — — — Stations 1, 2B, 3B, 4

Table 4.1: Tracking Station Coordinates

WGS 72 and Conventional Terrestrial Datums

Station	Lat. (°) x (m)	Long. (°) y (m)	Ht. (m) z (m)
1 Dominion Radio Astrophysical Observatory	49.42 -2060856.12	-119.65 -3620402.85	547.5 4814245.35
2A Yellowknife Seismic Station	62.47 -1225808.90	-114.50 -2689792.14	203.9 5633096.01
2B Repulse Bay	67.00 174343.21	-86.00 -2493224.10	200.0 5848595.82
3A Algonquin Radio Observatory	45.95 917575.63	-78.08 -4346688.12	240.0 4561556.48
3B Houston Texas	30.0 -577887.14	-96.00 -5498228.89	300.0 3170522.92
4 Port Blanford Nfld.	48.30 2492049.90	-54.11 -3443897.21	152.0 4739244.38

The ellipsoid coordinates are referred to the WGS 72 datum and the Cartesian coordinates are in the conventional terrestrial system [Vanicek and Krakiwsky, 1982]. The first network chosen, network A, was collocated with four stations of the proposed Canadian Long-Baseline Array (CLBA) [Canadian Astronomical Society, 1984]. This network was selected to locate the stations over as large an extent as possible, while still retaining the stations in Canadian territory. CLBA stations were chosen since accurate station coordinates would be readily available, as shown in the results of Shapiro [1979] where relative station accuracies on the order of 1 part in 10^{-8} were obtained using VLBI and laser ranging techniques. The result, however, is a network with a large east/west extent but a much smaller north/south extent. The possibility of this limiting geometric aspect to network A affecting orbit improvement solutions was recognized, and network B was selected so a comparison could be carried out. In network B, station 2 was moved further north and station 3 was moved south to Houston Texas, resulting in a much larger north/south extent.

The effect of inaccuracy in tracking station coordinates on orbit improvement solutions was studied, and these results will be presented in Chapter 5. The tests involved increasing the a priori standard deviations on the coordinates and applying random errors to the coordinate values until the orbit solution degraded beyond the desired level of accuracy. The use of accurate frequency standards at all tracking stations is also essential for orbit computations. The method for treating clock error outlined in Varnum and Chaffee [1982] was adopted, where cesium fequency standards are used at each tracking station. The procedure involves solving for a time offset (bias) and drift for each station clock, except one station designated as establishing the master time scale.

4.2 Simulation of Observations

The analyses carried out in this study were done with simulated observations. The observations were simulated using the program DIFGPS, developed at The University of New Brunswick [Davidson et al., 1983]. The program was modified by the author to use the orbit integration package PEGS for computing satellite positions. Further modifications were carried out to generate data files compatible with the adjustment program ASTRO.

The observation types generated were pseudorange, continuously integrated Doppler (CID), and single difference phase (SD). In certain tests the observations were generated with random error applied using a random number generator and one sigma standard deviations of 2 m for pseudoranges and 0.1 m for CID and SD. These accuracies reflect receiver random error, atmospheric modeling error, satellite group delay and multipath effects, and are taken from Martin [1978]. These one sigma values do not include inaccuracy due to satellite position error and oscillator instability. Instead, satellite reference initial conditions and clock polynomial coefficients are treated as weighted parameters in the least squares adjustment, and their inaccuracy is explicitly propagated into the solution using a priori covariance information.

Pseudorange and CID observations were simulated at 60 second intervals for orbit improvement tests, while the SD interval used was 80 seconds. This resulted in approximately 900 observations to each four hour satellite pass. Station coordination tests were carried out using pseudorange and CID observations at 180 second intervals and SD observations at 240 second intervals. These intervals produced approximately 300 observations per pass, however three passes were processed simultaneously resulting in approximately 900 observations per station solution.

In certain cases the observations were simulated with receiver clock biases. The details of these tests will be given in Chapters 5 and 6. The satellite reference initial conditions used to simulate observations define the 'correct' orbit. The a priori satellite initial conditions used in the adjustment process were varied, again depending upon the specific test being done.

4.3 Simulation Procedure

The ability to solve errors in orbit elements was tested by applying an error to the reference initial conditions used to simulate observations. The errors applied were usually 50 m (1.8×10^{-6} radians), however, smaller errors of 10 m were used in some cases. The biased orbit elements were then used as a priori values in the adjustment prosess, with their a priori standard deviations increased to a level commensurate with the error applied. A least squares adjustment was then performed using the simulated observations to recover the correct initial conditions.

The orbit improvement tests were carried out for three different satellite passes, and for each observation type independantly. Tests were done for one orbit element at a time, and then multiple elements were solved simultaneously. Certain multiple element tests were repeated using pseudorange and CID observations to network B in order to test the effect of network geometry on orbit improvement capabilities.

The solution of receiver clock errors simultaneously with either orbit errors or station coordinates was studied using procedures similar to the orbit improvement tests. The observations from tracking network A were simulated with clock biases on stations 1, 2A and 3A. Orbit solutions were carried out while simultaneously solving for these clock errors, using a priori values of zero for the biases. The solution of clock drifts was tested by using non-zero a priori drift values for stations 1, 2A and 3A, while the observations were simulated with zero drifts.

Solutions for station coordinates on a local scale were carried out to compare the accuracy of results when using a broadcast orbit versus an improved orbit. In all cases the a priori coordinates for two of the three stations were put in error by 500 m . The comparison was done by first solving for the station coordinates using a priori satellite initial conditions in error and held fixed. The incorrect initial conditions were then improved using tracking network A observations, then the local station solution was repeated with the improved orbit. Finally, the local station solution was performed using the incorrect initial conditions, however correct a priori standard deviations were used to attempt a simultaneous orbit improvement and station solution.

The results of all tests described in this section are presented in the following two chapters. Table 4.2 gives a summary of the simulation tests carried out.

Table 4.2: Summary of Tests

Parameters Solved	Purpose of Test
• single orbit elements	• test force model and adjustment formulation • test computer coding of above
• multiple orbit elements	• analyze ability to do orbit improvement over Canada for the three observation types • comparison of network configurations • study effect of inaccuracy in tracking station coordinates
• multiple orbit elements and clock error	• test ability to resolve clock and orbit error simultaneously
• station coordinates and clock error	• test ability to resolve station coordinate and clock error simultaneously
• station coordinates and orbit error	• study effect of orbit error on station coordinate solutions • compare station positioning using broadcast versus improved orbits

CHAPTER 5

RESULTS - ORBIT IMPROVEMENT

The simulation results presented in this chapter demonstrate the capability of doing short-arc orbit improvement over Canada. The first set of results given in section 5.1 are for single and multiple orbit element errors using pseudorange, CID and SD observations from network A. In section 5.2 the results of multiple orbit element error tests are given for observations from network B. The next set of results, presented in section 5.3, are for the solution of receiver clock errors simultaneously with orbit element errors. Finally, in section 5.4, the results of tests on the effect of inaccuracy in the tracking station coordinates on orbit improvement are presented.

5.1 Network A Results

Tests were carried out using observations from network A to determine how well errors in orbit elements could be recovered. The tests were done for three satellite passes over Canada, each having a four hour duration, with errors on single elements solved individually and then in various combinations. The results of these tests have been presented previously in Nakiboglu et al. [1985].

The first set of tests performed were done with perfect observations. No random observational error was applied in order to test the satellite force model and adjustment formulation under perfect conditions. In each test the a priori value for one orbit element was put in error by 50 m (1.8×10^{-6} radian), and its a priori standard deviation was also increased to this level. Pseudorange and CID observations were simulated at 60 second intervals, producing approximately 900 observations per pass. The interval for SD observations was increased to 80 seconds so that approximately the same number of observations were generated. This type of test was carried out separately for each Keplerian orbit element and for the three different satellite passes over Canada. Using pseudorange observations, the maximum error remaining in an orbit element after the solution converged was 0.02 m, and generally the remaining error was 0.01 m or less. The one sigma standard deviations for these solutions ranged from 0.09 to 1.36 m, and were generally on the order of 0.60 m. The maximum error remaining in CID solutions was 0.12 m, and again was generally 0.01 m or less. The standard deviations ranged from 0.01 to 0.11 m. The SD solutions had a maximum error of 0.35 m, and the standard deviations ranged from 0.06 to 0.37 m. The convergence tolerance used to stop the adjustment from iterating was 1.0 m for corrections to the orbit elements, indicating the adjustment formulation and force model are programmed and working correctly.

The next set of tests performed were done in the same manner as the single element tests, except multiple elements were put in error and solved simultaneously. The pseudorange, CID and SD results for these tests are given in Tables 5.1, 5.2 and 5.3 respectively.

Table 5.1: Multiple Orbit Element Errors
Pseudorange Solutions

Elements Biased by 50 Metres	Error Remaining in Elements[3]	σ of Elements	MSCCE[1]	ASCCE[2]
a	0.24	0.14		
e	0.02	0.30	0.6	0.2
M	0.46	1.62		
a	0.00	0.10		
i	0.00	1.32	0.5	0.2
M	0.00	0.60		
a	0.00	0.10	0.5	0.3
M	0.00	0.59		
a	0.00	0.10		
Ω	0.01	2.83	0.6	0.3
M	0.00	1.70		
a	0.24	0.16		
e	0.04	0.46	1.1	0.3
i	0.12	2.03		
Ω	1.30	2.98		
M	1.28	3.03		
a	0.00	0.11		
ω	0.01	1.78	0.3	0.2
i	0.01	1.40		
Ω	0.01	2.98		

1 MSCCE = Maximum satellite Cartesian coordinate error.

2 ASCCE = Average satellite Cartesian coordinate error.

3 As mentioned previously, the tolerance used to stop the adjustment from iterating was 1.0 m . The remaining errors below 1 m will decrease and may actually become zero if the adjustment was iterated further with a lower convergence tolerance. Errors larger than 1 m would not likely be completely removed since the corrections have already fallen below this level. The larger remaining errors are due to ill-conditioning in the adjustment and truncation errors introduced by the analytical formulation.

Table 5.2: Multiple Orbit Element Errors
CID Solutions

Elements Biased by 50 Metres	Error Remaining in Elements (m)	σ of Elements (m)	MSCCE (m)	ASCCE (m)
a	0.70	0.03		
e	0.15	0.04	1.7	0.4
M	0.43	0.27		
a	0.00	0.03		
i	0.00	0.19	0.0	0.0
M	0.01	0.16		
a	0.00	0.03	0.0	0.0
M	0.01	0.16		
a	0.00	0.03		
Ω	0.01	0.15	0.0	0.0
M	0.01	0.18		
a	0.66	0.22		
e	0.01	0.08	1.2	0.5
i	0.82	0.43		
Ω	0.60	0.29		
M	1.54	0.40		
a	0.00	0.03		
ω	0.01	0.18	0.0	0.0
i	0.01	0.25		
Ω	0.00	0.19		

Table 5.3: Multiple Orbit Element Errors
SD Solutions

Elements Biased by 50 Metres	Error Remaining in Elements (m)	σ of Elements (m)	MSCCE (m)	ASCCE (m)
a	0.21	0.08		
e	0.06	0.28	0.8	0.4
M	1.61	0.72		
a	0.09	0.08		
i	0.06	0.32	1.4	0.6
M	0.10	0.32		
a	0.10	0.06	0.6	0.4
M	0.07	0.30		
a	0.20	0.11		
Ω	0.16	0.22	0.8	0.4
M	1.12	0.32		
a	0.67	0.19		
e	0.85	0.44	2.0	0.8
i	1.27	0.42		
Ω	0.34	0.28		
M	0.29	1.08		
a	0.27	0.11		
ω	0.13	0.35	1.0	0.8
i	0.78	0.33		
Ω	0.03	0.23		

The results of these three sets of tests indicate it is possible to resolve errors of 50 m in multiple orbit elements using the three observation types separately. The maximum error remaining in the orbit elements is on the order of 1.2 to 1.5 m when five elements are solved for simultaneously. The level of error in the satellite Cartesian coordinates is approximately the same as the error in the orbit elements. The accuracy of the pseudorange solutions are satisfactory, but generally they are poorer than CID and SD solutions. This difference can be attributed to the higher level of random error associated with GPS pseudorange observations.

5.2 Network B Results

The north/south extent of network A is limited since the stations are located at CLBA sites. This limitation may have an affect on the orbit improvement solutions, therefore network B was selected so comparisons could be made.

Certain multiple orbit element error tests performed using pseudorange and CID observations from network A were repeated using network B. The results of these tests are given in Tables 5.4 and 5.5 for pseudorange and CID observations respectively. The network B tests were not done with SD observations, since these results are similar to CID results.

Table 5.4: Network B - Pseudorange Solutions

Elements Biased by 50 Metres	Error Remaining in Elements (m)	σ of Elements (m)	MSCCE (m)	ASCCE (m)
a	0.00	0.10		
i	0.00	1.24	0.5	0.2
M	0.00	0.59		
a	0.24	0.14		
Ω	0.01	0.26	0.4	0.2
M	0.41	1.34		
a	0.24	0.13		
e	0.02	0.27	0.5	0.3
i	0.12	1.26		
Ω	0.27	2.70		
M	0.58	2.11		
a	0.00	0.11		
ω	0.01	1.56	0.4	0.2
i	0.00	1.24		
Ω	0.01	2.68		

Table 5.5: Network B - CID Solutions

Elements Biased by 50 Metres	Error Remaining in Elements (m)	σ of Elements (m)	MSCCE (m)	ASCCE (m)
a	0.68	0.03		
e	0.20	0.03	1.4	0.4
M	0.07	0.18		
a	0.00	0.03		
i	0.01	0.20	0.0	0.0
M	0.01	0.15		
a	0.68	0.04		
e	0.11	0.06	1.5	0.4
i	1.04	0.35		
Ω	0.20	0.25		
M	0.60	0.26		
a	0.00	0.04		
ω	0.00	0.15	0.0	0.0
i	0.00	0.22		
Ω	0.00	0.18		

The network B pseudorange and CID results presented in Tables 5.4 and 5.5 are only marginally better than the network A results given in Tables 5.1 and 5.2 . These results indicate that the greater north/south extent of network B affords only a slight increase in orbit improvement capabilities over Canada, and that network A is sufficient. It should be noted, however, that although these tests were performed using three different satellite passes, network B may show greater strength in resolving errors in other satellite arcs not tested.

5.3 Receiver Clock and Orbit Error Solutions

The use of accurate and stable frequency standards is necessary at tracking stations for GPS orbit improvement, however time offsets and drifts in the receiver oscillators will inevitably be present. At GPS master control, where satellite orbits and clock states are predicted and uploaded to the satellites, an offset and drift term is determined for each tracking station clock relative to one master station [Varnum and Chaffee,1982]. This approach was applied and investigated in this study.

Four test runs were done using pseudorange observations from network A. The observations were simulated with receiver clock biases of 1.1, 1.2 and 1.3 seconds on stations 1, 2 and 3 respectively. Random error was also applied to the observations, using a random number generator and standard deviation of 2.0 m . Random observational error was used for these tests since their affect may be more noticeable in the presence of clock errors. The resulting orbit solutions should also be more realistic when the simulated observations are perturbed. The first test involved an orbit improvement solution only, with the correct a priori clock bias values used and weighted heavily. In the second test, the correct orbit initial conditions were input and a priori values of zero were used for the clock biases. The results of these two tests are given in Table 5.6 .

Table 5.6: Orbit and Receiver Clock Error Solutions

Run 1 - Orbit solution, biases known

Elements Biased by 50 Metres	Error Remaining in Elements (m)	σ of Elements (m)	MSCCE (m)	ASCCE (m)
a	0.11	0.11		
ω	1.54	1.73	1.4	0.5
i	1.34	1.38		
Ω	1.93	2.88		

Run 2 - Bias solution, orbit known

Station	Error Remaining in Bias (sec)	σ of Bias (sec)	MSCCE (m)	ASCCE (m)
1	0.0×10^{-9}	0.54×10^{-9}		
2	0.0×10^{-9}	0.51×10^{-9}	0.0	0.0
3	1.0×10^{-9}	0.46×10^{-9}		

The orbit improvement solution given in Table 5.6 is consistent with results presented earlier, however the errors remaining in orbit elements are now of the same magnitude as the standard deviations of the solutions. This result occurs since random error has now been applied to the observations. The results of run 2 indicate large time bias errors can be solved to a satisfactory level of accuracy.

The next test performed was a simultaneous solution of the orbit and time bias errors used in runs 1 and 2. This test was then repeated, with a priori clock drifts of 11.0×10^{-9}, 12.0×10^{-9} and 13.0×10^{-9} $\mathrm{sec \cdot sec^{-1}}$ imposed on stations 1, 2 and 3 respectively. The a priori drift standard deviations were also increased to this level, to determine if the correct zero drift values could be recovered with the clock bias and orbit errors. The results of these two tests are given in Tables 5.7 and 5.8 respectively.

Table 5.7: Orbit and Clock Bias Solutions

Elements Biased by 50 Metres	Error Remaining in Elements (m)	σ of Elements (m)	MSCCE (m)	ASCCE (m)
a	0.02	0.17		
ω	0.60	2.19	3.5	1.8
i	3.79	4.13		
Ω	0.95	3.43		

Station	Error Remaining in Bias (sec)	σ of Bias (sec)
1	0.0×10^{-8}	1.3×10^{-9}
2	0.2×10^{-8}	1.5×10^{-9}
3	0.0×10^{-8}	6.2×10^{-9}

Table 5.8: Orbit and Clock Bias/Drift Solutions

Elements Biased by 50 Metres	Error Remaining in Elements (m)	σ of Elements (m)	MSCCE (m)	ASCCE (m)
a	0.02	0.26		
ω	2.20	4.36	3.5	1.8
i	4.30	6.36		
Ω	3.81	7.08		

Station	Error Remaining in Bias (sec)	σ of Bias (sec)	Error in Drift ($sec \cdot sec^{-1}$)	σ of Drift ($sec \cdot sec^{-1}$)
1	1.0×10^{-9}	3.9×10^{-9}	0.8×10^{-13}	4.1×10^{-13}
2	3.0×10^{-9}	4.4×10^{-9}	1.3×10^{-13}	4.0×10^{-13}
3	0.0×10^{-9}	1.1×10^{-9}	0.6×10^{-13}	1.4×10^{-13}

The results presented in Tables 5.7 and 5.8 indicate receiver clock biases and drifts can be solved simultaneously with orbit errors. The satellite Cartesian coordinate error is at an acceptable level, however the

Keplerian element solutions are poorer. The discrepancy may occur from a compensating effect in the Keplerian errors, resulting in more accurate Cartesian coordinates. This drop in the accuracy of orbit elements when they are solved simultaneously with clock biases and drifts may be overcome by using more than one observation type simultaneously in the solution.

5.4 Effect of Inaccuracy in Tracking Station Coordinates

The ability to improve GPS orbits to a 2.5 m level of accuracy implies an accurate network of tracking stations exists. The results presented so far were obtained from tracking stations constrained with a priori coordinate standard deviations of 0.001 m (ie. in effect the stations were held fixed). Simulation tests were carried out to determine at what level station coordinate inaccuracy would corrupt the orbit solution beyond the 2.5 m level.

The tests were performed using pseudorange and CID observations from network A, with random observation error applied. First, an orbit solution was done with the tracking station coordinates held fixed. Next, the orbit solution was repeated with a priori station coordinate standard deviations increased in steps until the orbit solution degraded beyond 2.5 m in accuracy. Random error was also applied to the station coordinate values commensurate with the standard deviations used. This procedure of increasing a priori standard deviations and corrupting the coordinates was only applied to stations 1, 3A and 4 in the network, allowing for the computation of relative station accuracies with respect to station 2A. The results of these pseudorange and CID tests are given in Tables 5.9 and 5.10 respectively.

Table 5.9: Tracking Station Inaccuracy Pseudorange Solutions

Elements Biased by 50 Metres	Error Remaining in Elements (m)	σ of Elements (m)	MSCCE (m)	ASCCE (m)
Run 1 - Station coordinate σ = 0.001 m				
a	0.41	0.14		
e	0.35	0.30	0.8	0.6
M	1.03	1.62		
Run 2 - Stations 1,3,4 coordinate σ = 0.100 m				
a	0.40	0.16		
e	0.33	0.35	1.8	0.6
M	0.87	1.88		
Run 3 - Stations 1,3,4 coordinate σ = 0.500 m				
a	0.87	0.39		
e	1.14	0.78	6.6	2.8
M	5.34	4.19		

Table 5.10: Tracking Station Inaccuracy
CID Solutions

Elements Biased by 50 Metres	Error Remaining in Elements (m)	σ of Elements (m)	MSCCE (m)	ASCCE (m)
Run 1 - Station coordinate σ = 0.001 m				
a	0.00	0.03		
ω	0.01	0.19	0.0	0.0
i	0.03	0.25		
Ω	0.03	0.20		
Run 2 - Stations 1,3,4 coordinate σ = 0.100 m				
a	0.13	0.09		
ω	0.06	0.23	0.5	0.3
i	0.44	0.57		
Ω	0.64	0.63		
Run 3 - Stations 1,3,4 coordinate σ = 0.500				
a	0.26	0.33		
ω	0.61	0.41	2.9	1.5
i	2.05	1.77		
Ω	2.77	2.53		

The relative accuracy of tracking stations is determined using the relation

$$\text{Relative Accuracy} = \sigma_d d^{-1}, \tag{5.1}$$

where

d is the distance between stations,

$\sigma_d = \sqrt{\sigma_x^2+\sigma_y^2+\sigma_z^2}$, and

$\sigma_d, \sigma_x, \sigma_y$ and σ_z are standard deviations of distance d, and coordinates x,y,z respectively. It should be noted that the standard deviation of x is equal to that of Δx between two stations in this case, since one station is considered known (fixed). The accuracy of tracking stations relative to station 2A, computed using Equation 5.1, are given in Table 5.11

Table 5.11: Relative Accuracy of Tracking Stations

Station	Distance to Station 2A (km)	Relative Accuracy for $\sigma_x=\sigma_y=\sigma_z=0.10$ m (ppm)	Relative Accuracy for $\sigma_x=\sigma_y=\sigma_z=0.50$ m (ppm)
1	1500	0.12	0.58
3	2900	0.06	0.30
4	3900	0.04	0.22

The results of tests on tracking station coordinate accuracy indicate that relative accuracies on the order of 0.1 ppm are required to insure the orbit improvement solution is not corrupted. These results tend to confirm the conclusions of Stolz et al. [1984].

CHAPTER 6

RESULTS - STATION COORDINATION

The use of GPS observations for determining station coordinates and coordinate differences has become a common practice, even though the satellite system is not yet fully operational. The standard solution method involves solving for station coordinates (or coordinate differences) and an offset for the receiver clock relative to GPS time. Simulated tests were performed for the solution of station coordinates and clock errors independently and simultaneously. These tests were done with satellite orbit error propagated into the solution, and the results are given in section 6.1 . The final set of tests performed for this study was a comparison of station positioning results with a broadcast orbit accuracy versus an improved orbit. The method used to do this comparison and the corresponding results are given in section 6.2 .

6.1 Station Coordinate and Clock Error Solutions

The test results presented in this section were obtained using pseudorange and SD observations from three satellite passes to three local stations. The pseudorange observations were simulated at 3 minute intervals with random error applied at a 2 m level, while the SD observations had an interval of 4 minutes and a 0.1 m level of random error. This procedure yielded approximately 240 observations per pass from the three stations, or approximately 80 observations per station to each satellite pass. The station locations are given in Table 6.1

Table 6.1: Local Station Positions

WGS 72 and Conventional Terrestrial Datums

Station	Lat. (°) x (m)	Long. (°) y (m)	Ht. (m) z (m)
1 Saskatoon	52.20 -1147923.40	253.00 -3754688.25	100.0 5009723.60
2 Edmonton	53.50 -1516128.26	246.50 -3486856.28	200.0 5103996.84
3 Calgary	51.1 -1635663.40	245.9 -3665148.93	300.0 4940770.35

The first two pseudorange tests involved the solution of receiver clock biases and drifts only. In run 1, a priori bias values for stations 2 and 3 were input incorrectly by 1.2 and 1.3 seconds respectively, with a priori standard deviations increased accordingly. The second test was a repeat of run 1, with station 2 and 3 a priori drifts input with 12×10^{-9} and 13×10^{-9} $sec \cdot sec^{-1}$ errors respectively. In both tests, a priori satellite covariance matrices were used to propagate orbit error into the solution. Standard deviations of 1 m were used for the semi-major axis, inclination and right ascension, and 20 m for the argument of perigee. The results of these two tests are given in Table 6.2 .

Table 6.2: Local Station Clock Bias/Drift Solutions

Station	Error Remaining in Bias (sec)	σ of Bias (sec)	Error in Drift ($sec \cdot sec^{-1}$)	σ of Drift ($sec \cdot sec^{-1}$)
Run 1 - Bias solution				
2	0.85×10^{-9}	0.6×10^{-9}		
3	0.12×10^{-9}	0.6×10^{-9}		
Run 2 - Bias and drift solution				
2	0.16×10^{-9}	1.2×10^{-9}	1.0×10^{-13}	1.0×10^{-13}
3	0.34×10^{-9}	1.2×10^{-9}	0.2×10^{-13}	1.0×10^{-13}

The results given in Table 6.2 indicate that bias and drift solutions are possible for the network of three local stations, however, these tests were done with correct station coordinates. The test performed in run 2 was repeated, with 500 m errors on the coordinates of stations 2 and 3. The results of this test are given in Table 6.3.

Table 6.3: Clock Bias/Drift and Station Coordinate Solutions

Station	Error Remaining in Bias (sec)	σ of Bias (sec)	Error in Drift ($sec \cdot sec^{-1}$)	σ of Drift ($sec \cdot sec^{-1}$)
2	0.6×10^{-9}	2.6×10^{-9}	4.0×10^{-14}	13.0×10^{-14}
3	1.8×10^{-9}	2.5×10^{-9}	0.9×10^{-14}	13.0×10^{-14}

Station	Errors Remaining in Coordinates x (m)	y (m)	z (m)	σ of Coordinates x (m)	y (m)	z (m)
2	0.03	0.22	0.37	0.42	0.72	0.64
3	0.02	0.67	0.47	0.43	0.71	0.62

The clock bias and drift solutions are slightly poorer when done simultaneously with station coordinates, however, they are still acceptable. The distances from station 1 to stations 2 and 3 are approximately 464 and 500 km respectively. Applying Equation 5.1, the relative accuracies on these two lines are 2.3 and 2.1 ppm respectively. This accuracy for station positioning is realistic, given the level of orbit error propagated into the solution.

The last two tests using pseudorange observations and clock errors also involved an along-track satellite orbit error. The orbit error was imposed by applying a 20 m error to the a priori argument of perigee values for each satellite. In the first test, the satellite orbits were held fixed with large a priori weights, allowing the orbit error to be absorbed into the coordinate solutions. In the second test, correct a priori standard deviations were used for the satellite orbit elements. The results of these two tests are given in Tables 6.4 and 6.5 respectively.

Table 6.4: Along-track Orbit Error Held Fixed

Station	Error Remaining in Bias (sec)	σ of Bias (sec)	Error in Drift ($sec \cdot sec^{-1}$)	σ of Drift ($sec \cdot sec^{-1}$)
2	3.0×10^{-9}	2.3×10^{-9}	9.0×10^{-14}	9.8×10^{-14}
3	5.8×10^{-9}	2.2×10^{-9}	0.1×10^{-14}	9.7×10^{-14}

Station	Errors Remaining in Coordinates			σ of Coordinates		
	x (m)	y (m)	z (m)	x (m)	y (m)	z (m)
2	4.09	2.15	2.13	0.32	0.61	0.56
3	4.29	1.76	2.99	0.32	0.61	0.54

Table 6.5: Along-track Orbit Error
Correct Weights

Station	Error Remaining in Bias (sec)	σ of Bias (sec)	Error in Drift ($sec \cdot sec^{-1}$)	σ of Drift ($sec \cdot sec^{-1}$)
2	0.6×10^{-9}	2.6×10^{-9}	3.3×10^{-14}	13.0×10^{-14}
3	1.8×10^{-9}	2.5×10^{-9}	1.5×10^{-14}	13.0×10^{-14}

Station	Errors Remaining in Coordinates			σ of Coordinates		
	x (m)	y (m)	z (m)	x (m)	y (m)	z (m)
2	0.01	0.22	0.36	0.42	0.72	0.64
3	0.01	0.67	0.48	0.43	0.71	0.62

The results in Table 6.4 indicate that an orbit error adversely affects the solution, when the error is held fixed. The clock bias and drift solutions are only slightly worse, whereas the station coordinate solutions have absorbed most of the orbit error and are significantly worse. The results in Table 6.5 show that using correct a priori weights on the satellite orbit results in the correct solution. This is evident from a comparison of Table 6.5 with Table 6.3. The two sets of results are nearly identical. Using correct weights for the along-track orbit error of 20 m enabled the solution of these errors. The remaining error in the argument of perigee for the three satellites used ranged from 0.5 to 2.8 m .

The tests performed with SD observations involved the solution of clock drifts with station coordinates. The affect of clock biases on the station coordinate solutions was tested in a manner similar to that used by Remondi [1984], where a clock bias error is input but not recovered in the adjustment. The same a priori satellite covariance matrices used in the previous pseudorange tests were again used, in order to propagate orbit inaccuracy into the solution covariance matrix.

In the first test, an a priori bias of 50 microseconds (50×10^{-6} sec) was input for stations 2 and 3. Clock drift values of 1.2×10^{-6} and 1.3×10^{-6} $sec \cdot sec^{-1}$ were used for stations 2 and 3 respectively, where the actual values should be zero. The solution for the drifts had remaining errors of 5.2×10^{-15} and 4.9×10^{-15} $sec \cdot sec^{-1}$ for stations 2 and 3 respectively, and corresponding standard deviations of 9.2×10^{-15} and 9.7×10^{-15} $sec \cdot sec^{-1}$. These results are acceptable, and the existence of 50 microsecond bias errors did not severely affect the solution. This same test was repeated, with stations 2 and 3 coordinates in error by 500 m . The results of this test are given in Table 6.6 .

Table 6.6: Clock Drift and Station Coordinate Solution

Station	Error Remaining in Drift ($sec \cdot sec^{-1}$)	σ of Drift ($sec \cdot sec^{-1}$)
2	2.0×10^{-14}	4.9×10^{-14}
3	0.2×10^{-14}	4.7×10^{-14}

Station	Errors Remaining in Coordinates			σ of Coordinates		
	x (m)	y (m)	z (m)	x (m)	y (m)	z (m)
2	0.05	0.01	0.04	0.18	0.05	0.10
3	0.01	0.02	0.01	0.19	0.06	0.09

The solution for clock drifts in Table 6.6 are slightly poorer than when coordinate errors were not present, however the results are still satisfactory. The station coordinates were recovered with an accuracy, relative to station 1, of 0.5 and 0.4 ppm for stations 2 and 3 respectively. These results are slightly optimistic, and again the clock biases did not affect the results to a large degree. This level of clock bias error not corrupting the station coordinate solution agrees with the conclusions of Remondi [1984].

The last two tests carried out for SD observations were on the effect of orbit errors. In the first test, a 20 m error in the argument of perigee was imposed on each satellite and held fixed in the solution. The same coordinate and clock errors used for the results in Table 6.6 were used. This test was then repeated, with the correct a priori weighting on the satellite orbit elements. The results of these two tests are given in Tables 6.7 and 6.8 respectively.

Table 6.7: Along-track Orbit Error Held Fixed

Station	Error Remaining in Drift (sec•sec^{-1})	σ of Drift (sec•sec^{-1})
2	5.6×10^{-14}	3.6×10^{-14}
3	9.7×10^{-14}	3.6×10^{-14}

Station	Errors Remaining in Coordinates			σ of Coordinates		
	x (m)	y (m)	z (m)	x (m)	y (m)	z (m)
2	0.17	0.11	0.37	0.12	0.03	0.07
3	0.58	0.11	0.31	0.12	0.03	0.07

Table 6.8: Along-track Orbit Error
Correct Weights

Station	Error Remaining in Drift (sec•sec^{-1})	σ of Drift (sec•sec^{-1})
2	1.7×10^{-14}	4.9×10^{-14}
3	1.0×10^{-14}	4.7×10^{-14}

Station	Errors Remaining in Coordinates			σ of Coordinates		
	x (m)	y (m)	z (m)	x (m)	y (m)	z (m)
2	0.04	0.01	0.01	0.18	0.05	0.10
3	0.08	0.01	0.04	0.19	0.06	0.09

The results in Table 6.7 show how the orbit error, when held fixed, affects the station coordinate solution. The effect, however, is much less severe for SD observations than for pseudorange observations, as seen by comparing Tables 6.7 and 6.4 . This result is expected, since SD observations are used to minimize the effect of orbit errors by partially canceling their effect via the differencing technique. The results in Table 6.8 show how correct weighting improves the solution to the level of error seen in Table 6.6, where no orbit error was imposed. The error remaining in the argument of perigee was on the order of 4 to 5 metres using the SD observations. The orbit error was not recovered to the same level of accuracy as in the pseudorange solutions, but again the SD observations are not as sensitive to these errors.

6.2 Broadcast Versus Improved Orbits

The simulations were carried out for this section to show how improvement in positioning accuracy results when using an improved orbit versus a broadcast orbit having a higher level of error. The tests were performed with pseudorange and CID observations under the same conditions described in section 6.1 . The solution representing a broadcast orbit was done with 10 m errors on the semi-major axis, inclination and right ascension, and with a 50 m error on the argument of perigee. These errors were applied to the three satellite passes used, and the orbit elements were held fixed during the station solution. The pseudorange and CID solutions for these two tests are given in Table 6.9 .

Table 6.9: Solutions with Broadcast Orbit

Station	Errors Remaining in Coordinates x (m)	y (m)	z (m)	σ of Coordinates x (m)	y (m)	z (m)
Run 1 - pseudorange solution						
2	4.96	1.17	7.00	0.31	0.23	0.26
3	4.87	9.60	6.64	0.32	0.23	0.25
Run 2 - CID solution						
2	3.28	1.76	1.43	0.04	0.04	0.03
3	2.73	1.71	1.23	0.04	0.04	0.03

The large errors in the station coordinates show the effect of orbit errors on the solution. The large discrepancy between the coordinate standard deviations and coordinate errors also implies that the weighting was incorrect in the adjustment, which is true since the orbits were held fixed. It should be noted that for this test, pseudorange observations were used and no clock errors were solved. In general, the effect of orbit errors would be lessened by using differenced observations, such as SD, DD or TD. When pseudoranges are used, a clock bias is usually solved which may absorb some along track orbit error, thereby improving the results. The test was carried out in the manner presented simply to emphasize the effect of orbit error, and to demonstrate the improvement when explicitly solving for orbit error.

The incorrect orbit elements were used as a priori values in an orbit improvement adjustment using network A. Two orbit solutions were done using pseudorange and CID observations independently, each having random error applied to the observations. The pseudorange improved orbit was then used to recompute the local station coordinates using pseudorange observations, and similarily the CID solution was repeated. The results of these improved orbit solutions are given in Table 6.10 .

Table 6.10: Solutions with Improved Orbit

Station	Errors Remaining in Coordinates			σ of Coordinates		
	x (m)	y (m)	z (m)	x (m)	y (m)	z (m)
Run 1 - pseudorange solution						
2	0.22	0.64	0.46	0.39	0.27	0.31
3	0.19	0.11	0.18	0.40	0.27	0.30
Run 2 - CID solution						
2	0.01	0.01	0.01	0.05	0.04	0.04
3	0.01	0.01	0.01	0.05	0.04	0.04

A comparison of Table 6.10 with 6.9 shows how the improved orbit yields a more accurate station solution. The coordinate errors are now of the same magnitude as the standard deviations of the solution.

The final test carried out for this study was a simultaneous solution of orbit errors and station coordinates. The tests done for the broadcast orbit were repeated, using the correct a priori covariance matrices to represent the level of orbit error present. The results of these tests are given in Table 6.11 .

Table 6.11: Simultaneous Station Solution and Orbit Improvement

Station	Errors Remaining in Coordinates			σ of Coordinates		
	x (m)	y (m)	z (m)	x (m)	y (m)	z (m)
Run 1 - pseudorange solution						
2	0.32	0.50	0.16	0.45	0.33	0.36
3	0.16	0.04	0.11	0.46	0.33	0.35
Run 2 - CID solution						
2	0.14	0.02	0.02	0.13	0.10	0.06
3	0.18	0.03	0.01	0.13	0.12	0.06

The results given in Table 6.11 are superior to those in Table 6.9, when the broadcast orbit was held fixed, but not as good as the results using an improved orbit given in Table 6.10 . These results are expected, since the orbit errors cannot be resolved as well from a local network of stations as compared to a larger network of national extent. The orbit error remaining in the pseudorange and CID solutions ranged from 0.09 to 16.08 m and 0.45 to 7.26 m respectively. It is encouraging, however, to see that orbit errors can be partially recovered simultaneously with station coordinates in the context of local positioning over several hundred kilometres.

CHAPTER 7

SUMMARY AND CONCLUSIONS

The main objective of this research, the development of a prototype multi-station, multi-pass GPS satellite data reduction program, has been met. The adjustment formulation in program ASTRO is a rigorous, weighted least squares approach. The ability to correct satellite reference initial conditions is incorporated into the adjustment to allow for orbit improvement capabilities. The program is also capable of solving for station coordinates, either on their own or simultaneously with corrections to satellite initial conditions. Program ASTRO utilizes the orbit integration package PEGS [Buffett, in prep.] to obtain satellite Cartesian coordinates.

7.1 Summary of Software Development

The software developed for this research consists of two program packages. The orbit integration software was developed by Buffett [in prep.], and is based on numerical integration of the equations of motion for the satellite to compute Cartesian coordinates. Analytical formulations are used to compute corrections to satellite Cartesian coordinates from corrections to reference initial conditions, rather than re-integrating an updated orbit. The program package ASTRO was developed by the author to do rigorous least squares adjustments using GPS observations, with the capability of doing orbit improvement either simultaneously or independently of station coordination. The observation types incorporated in the adjustment are pseudorange, continuously integrated Doppler, and single difference phase. The observation equations, defined in Chapter 2, include nuisance parameters representing satellite and receiver clock polynomial coefficients, unmodeled tropospheric refraction scale parameter, range bias for Doppler observations, and ambiguity parameters for single difference observations. All of these parameters, excluding the range bias and ambiguity parameters, are treated as weighted quantities in the adjustment allowing for proper a priori weights and estimates. A solar radiation pressure constant is also included as a weighted parameter.

The adjustment model, developed in Chapter 3, has a weighted least squares collocation form, with the unmodeled satellite perturbations modeled as a signal. The prototype program, however, does not have this signal component incorporated.

7.2 Conclusions

Two tracking network configurations, given in Chapter 4, were used to analyze orbit improvement capabilities over Canada. The results presented in Chapter 5 indicate that a 2.5 m level of accuracy is obtainable for satellite Cartesian coordinates, using an accurate, regional tracking network of four stations located in Canadian territory. The optimum network would be located at CLBA sites, where the required station positional accuracy of 0.1 ppm is easily obtained. The results also show the ability to recover receiver clock bias and drift errors simultaneously with orbit improvement.

Orbit improvement is possible with either of the three observation types used, however, an optimum solution would involve a combination of pseudorange with either

Doppler or single difference observations. The combination of observation types should strengthen the solution of nuisance parameters, such as clock errors, when solving for orbit errors. The method employed at GPS master control involves a combination of pseudorange and Doppler observations [Varnum and Chaffee, 1982].

The results presented in Chapter 6 show how the accuracy of local station coordinate solutions is increased when using an improved orbit, as compared to the accuracy when using a broadcast ephemeris. The results also show the ability to partially recover orbit errors when using broadcast orbits for local positioning on the order of a few hundred kilometres in station separation. This simultaneous recovery of orbit errors also improves the station solution accuracy.

7.3 Recommendations

The software developed to date has produced useful and interesting results, however, it is still a prototype package and utilizes simulated data. Extensions to this software package are recommended as follows :

1. The prototype package should be developed into a production package, utilizing actual GPS observations. This would require preprocessing input modules for

available observations, such as TI4100, Macrometer, etc. .

2. The software should be extended to include more thorough statistical testing, such as residual analysis and reliability analysis.
3. Adjustments should be performed with available data sets. If possible, data from a large tracking network should be used to further investigate orbit improvement.
4. The signal component of the adjustment model should be incorporated into the program and investigations carried out on the ability of this model to represent smaller perturbing effects.
5. The use of an orbit bias technique with GPS should be studied for local positioning and the results compared to results presented in section 6.2 .

REFERENCES

Anderle, R.J. (1982): Doppler test results of experimental GPS receiver. Naval Surface Weapons Center Report TR 82-01.

Beck, N., D. Delikaraoglou, K. Lochhead, D.J. McArthur, G. Lachapelle (1984): Preliminary results on the use of differential GPS positioning for geodetic applications. IEEE 1984 PLANS.

Beutler, G., D.A. Davidson, R.B. Langley, R. Santerre, P. Vanicek, D.E. Wells (1984): Some theoretical and practical aspects of geodetic positioning using carrier difference observations of GPS satellites. The University of New Brunswick Technical Report No.109.

Bock, Y., R.I. Abbott, C.C. Counselman III, R.W. King, S.A. Gourevitch (1985): Three-Dimensional geodetic control by interferometry with GPS : processing of GPS phase observables. Proceedings of The First Int. Symposium on Precise Positioning with the Global Positioning System, 255-262.

Brown, D.C. (1970): Near term prospects for positional accuracies of 0.1 to 1.0 metres from satellite geodesy. U.S. Air Force Cambridge Research Laboratories Report AFCRL-70-0501.

Buffett, B., in preparation: Short-arc orbit determination for the global positioning system. M.Sc. thesis, The University of Calgary.

Canadian Astronomical Society (1984): Collaborative options for the Canadian long baseline array.

Davidson, J.M., C.L. Thornton, C.J. Vegos, L.E. Young, T.P. Yunck (1985): The March 1985 demonstration of the fiducial network concept for GPS geodesy : a preliminary report. Proceedings of The First Int. Symposium on Precise Positioning with the Global Positioning System, 603-612.

Davidson, D., D. Delikaraoglou, R. Langley, B. Nickerson, P. Vanicek, D. Wells (1983): Global positioning system differential positioning simulations. The University of New Brunswick Technical Report No. 90.

Delikaraoglou, D. (1985): On error sources and mathematical models for use with GPS. Lecture notes for C.I.S. GPS Seminars, Calgary, May 7 1985.

Fell, P.J. (1980): Geodetic positioning using a global positioning system of satellites. Report No. 299 of the Department of Geodetic Science, The Ohio State University, Columbus, Ohio.

Goad, C.C., B.W. Remondi (1984): Initial relative positioning results using the global positioning system. Bulletin Geodesique, 58, 193-210.

Hopfield, H.S. (1971): Tropospheric effect on electromagnetic measured range : prediction from surface data. Radio Science, 6, 3, 357-367.

Krakiwsky, E.J., D.E. Wells (1971): Mathematical models for positioning by satellite. The University of New Brunswick Lecture Notes No. 17.

Lachapelle, G., E. Cannon (1985): GPS precise differential positioning over baselines of 300-500 km with a TI4100 receiver. C.I.S. Annual Meeting, Edmonton Alberta, May 28-31, 1985.

Martin, E.H. (1978): GPS user equipment error models. Navigation, 25, 2, 201-210.

Milliken, R.J., C.J. Zoller (1978): Principle of operation of NAVSTAR and system characteristics. Navigation, 25, 2, 95-106.

Moritz, H. (1972): Advanced least squares methods. Report No. 175 of the Department of Geodetic Science, The Ohio State University, Columbus, Ohio.

Nakiboglu, M., B. Buffett, K.P. Schwarz, E.J. Krakiwsky, B. Wanless (1984): A multi-station, multi-pass approach to GPS orbital improvement and precise positioning. IEEE PLANS 1984, 153-162.

Nakiboglu, S.M., E.J. Krakiwsky, K.P. Schwarz, B. Buffett, B. Wanless (1985): A multi-station, multi-pass approach to global positioning system orbital improvement and precise positioning. Final contract report OST83-00340, submitted to Geodetic Survey of Canada.

Remondi, B.W. (1984): Using the global positioning system (GPS) phase observable for relative geodesy: modeling, processing and results. Doctoral dissertation, University of Texas at Austin.

Schwarz, C.R. (1969): The use of short arc orbital constraints in the adjustment of geodetic satellite data. Report No. 118 of the Department of Geodetic Science, The Ohio State University, Columbus, Ohio.

Schwarz, K.P. (1976): Least squares collocation for large systems. Bollettino Di Geodesia E Scienze Affini 35, 3, 309-324.

Shapiro, I.I, C.C. Counselman, T.A. Herring (1979): Analysis of laser ranging and VLBI observations for geodetic purposes. Department of Earth and Planetary Physics, Massachussets Institute of Technology.

Spilker, J.J. (1978): Signal structure and performance characteristics. Navigation, 25, 2, 121-146.

Stolz, A., E.G. Masters, C. Rizos (1984): Determination of GPS satellite orbits for geodesy in Australia. Australian Journal Geod., Photo., Surv., 40, 41-52.

Van Dierendonck, A.J., S.S. Russell, E.R. Kopitzke, M. Birnbaum (1978): The GPS navigation message. Navigation, 25, 2, 147-165.

Vanicek, P., E.J. Krakiwsky (1982): Geodesy: the concepts. North Holland Publishing, Amsterdam.

Varnum, F., J. Chaffee (1982): Data processing at the global positioning system master control station. Proceedings of the Third Int. Geodetic Symposium on Satellite Doppler Positioning, 1023-1040.

Wells, D.E., E.J. Krakiwsky (1971): The method of least squares. The University of New Brunswick Lecture Notes No. 18.

Wells, D.E. (1974): Doppler satellite control. The University of New Brunswick Technical Report No. 29.

Wells, D.E., E.J. Krakiwsky, D.B. Thomson, J. Kouba (1976): Review of Doppler satellite positioning in Canada. Bulletin Geodesique, 50, 4, 307-322.